

sequences of HCV-KT9 with an alignment of the sequences of the 26 other genotype 1b strains. All HCV full-length clones reported from Japan were included in these 26 strains. Based on these comparisons, we identified 25 aa unique to HCV-KT9 (Fig. 2a). We found that the amino acid sequence of the IFN sensitivity-determining region in the NS5A region, which has been suggested to mediate IFN resistance via interaction with the cellular protein kinase R (Enomoto *et al.*, 1996; Gale *et al.*, 1997), was that of the wild-type.

Intrahepatic injection of HCV-KT1 and HCV-KT9 RNAs into human hepatocyte chimeric mice

In the next experiments, 30 µg *in vitro*-transcribed RNA of HCV-KT1, HCV-KT9 or HCV-KT9-GND was injected into the livers of chimeric mice. Eight of 10 (80%) HCV-KT9-injected mice developed measurable viraemia at 2 weeks post-inoculation (Table 1 and Fig. 3), with the HCV RNA titre reaching 1.1×10^6 to 8.8×10^6 copies ml⁻¹ at 6 weeks post-inoculation (Fig. 3). To check for the presence of infectious HCV in the serum of HCV-KT9-infected mice, each of five naïve mice was injected with 10 µl serum sample (containing 3.5×10^5 copies of HCV) obtained from an HCV-KT9-infected mouse 6 weeks after inoculation. All five naïve mice became positive for HCV RNA, as confirmed by nested PCR, at 2 weeks post-inoculation and two mice developed persistent viraemia (Fig. 4). These results indicated that the serum of HCV-KT9-injected mice contained infectious HCV. In contrast to HCV-KT9, none of the three mice injected with HCV-KT9-GND RNA developed viraemia (Table 1). These results indicated that HCV-KT9 replicates efficiently in mice livers and produces infectious virus continuously. On the other hand, only one out of seven HCV-KT1-injected mice (14%) developed measurable viraemia (Table 1 and Fig. 3). The level of viraemia was low in this HCV-KT1-infected mouse, HCV RNA was negative by nested PCR at 2 weeks after inoculation and the titre was only 2.2×10^4 copies ml⁻¹ at 4 weeks post-inoculation (Fig. 3). These results confirmed the importance of the poly(U/UC) tract length in experimentally induced viraemia.

The nucleotide and amino acid sequences of the viral genome isolated from an HCV-KT9-injected mouse (Fig. 3)

Table 1. Correlation between length of the poly(U/UC) tract and HCV infection

Clone	Length of poly(U/UC) tract	Number of mice			Infection ratio
		Infected	Not infected	Total	
HCV-KT1	86	1	6	7	14%
HCV-KT9	115	8	2	10	80%*
HCV-KT9-GND	115	0	3	3	0%

**P*=0.015, compared with HCV-KT1.

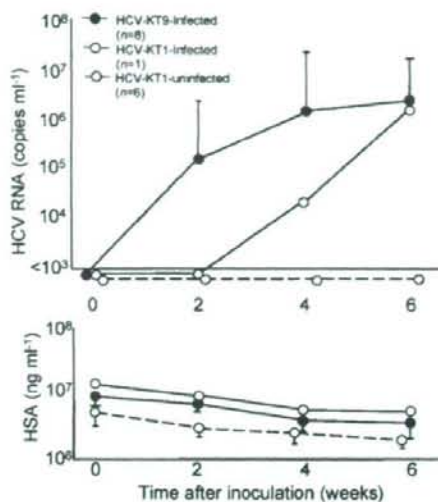


Fig. 3. Changes in HCV RNA levels and HSA concentrations in the sera of mice infected with clonal HCV. Mice were inoculated intrahepatically with 30 µg *in vitro*-transcribed HCV RNA. Eight of the ten HCV-KT9-infected mice (80%), one of the seven HCV-KT1-infected mice (14%) and none of the three HCV-KT9-GND-infected mice became positive for HCV RNA. The results for six HCV-KT1-uninfected mice are also shown. Mice serum samples were obtained every 2 weeks post-infection for analysis of HCV RNA titres. Data are shown as mean \pm SD.

at 6 weeks after RNA injection were identical to the injected HCV-KT9 (data not shown). We tried to reclone the poly(U/UC) tract in the HCV-KT1-infected mouse, but it was impossible to reamplify the HCV cDNA using the remaining small amount of serum.

Analysis of virus production from HCV-KT9-transfected cells

Next, we evaluated the ability of the HCV-KT9 clone to replicate in transfected Huh7 cells. In these experiments, we used JFH-1 RNA, which is known to replicate efficiently in cell cultures, as control (Wakita *et al.*, 2005). Core protein was secreted efficiently from JFH-1 RNA-transfected Huh7 cells. In contrast, we did not observe any measurable levels of core protein in the supernatant of HCV-KT9-transfected cells (Fig. 5), suggesting a minimal replication ability of HCV-KT9 to produce and release virus into the supernatant.

DISCUSSION

In this study, we described the establishment of a genotype 1b clone, HCV-KT9, that replicated efficiently following injection of the transcribed RNA into chimeric mouse liver.

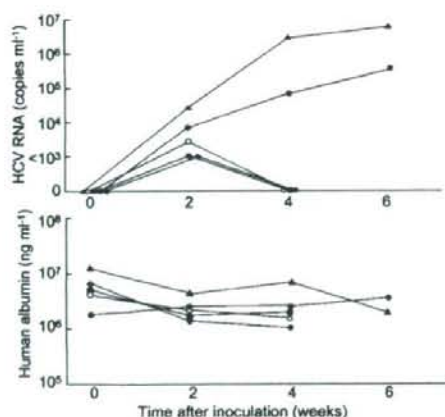


Fig. 4. Passage experiments of HCV in naive chimeric mice. Five naive chimeric mice were inoculated intravenously with 10 μ l serum sample (containing 3.5×10^5 copies HCV) obtained from an HCV-KT9-infected mouse at week 6 post-inoculation. Serum samples were obtained at the indicated time intervals for the measurement of HCV RNA levels and HSA concentrations. Data represent the changes in five individual mice.

The key factor that determines the infectivity of HCV clones has not yet been established. We previously established a clone from HCV that replicated in a chimeric mouse after injection of serum from a chronically HCV-infected patient. However, we did not observe viraemia after intrahepatic injection of the transcribed RNA from this clone (unpublished results). In contrast, injection of HCV-KT9 RNA in the present study resulted in viraemia in eight out of ten mice (80%). The fact that the nucleotide

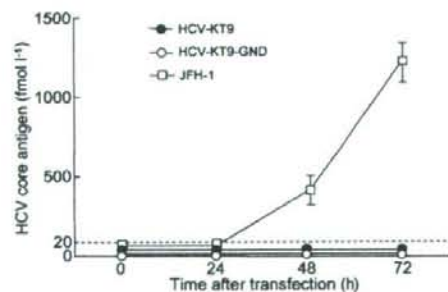


Fig. 5. Time-course studies of HCV core protein secretion into the culture medium of HCV RNA-transfected cells. Huh7 cells were transfected with 10 μ g HCV-KT9, HCV-KT9-GND or JFH-1 RNA. HCV core antigen in the culture medium was measured at 24, 48 and 72 h after transfection. Data are shown as mean \pm SD of HCV core protein levels obtained from three independent transfection experiments.

and amino acid sequences of the virus recovered from the infected mice were identical to those of the HCV-KT9 clone indicated that no adaptive mutation was necessary for this clone to replicate in the chimeric mouse.

Interestingly, the clone was obtained from a patient with severe acute hepatitis. This is similar to JFH-1, an HCV clone with a strong replication ability in cultured cell lines, chimpanzees and chimeric mice, which was cloned from serum samples of a patient who developed acute fulminant hepatitis with a high virus titre (Wakita *et al.*, 2005). A virus that replicates in the early stage of infection may have strong replication ability, which may be lost in the chronic phase of infection.

A key amino acid substitution may be present in one (or some) of the amino acids unique to this clone (Fig. 2a). We also showed that clone HCV-KT1, which differs from HCV-KT9 only in the length of the poly(U/UC) tract, had a poorer replication ability in mice (Table 1 and Fig. 3). However, there is a possibility that a shorter poly(U/UC) tract only slows down the rate of infection, as the HCV RNA titre in the HCV-KT1-infected mouse at 6 weeks after inoculation was similar to that in HCV-KT9-infected mice (Fig. 3). It has been reported that the length and composition of the poly(U/UC) tract is important for the replication of HCV replicons (Friebe & Bartenschlager, 2002; Yi & Lemon, 2003; You & Rice, 2008). However, no replication advantage of a poly(U/UC) tract longer than 86 bp was revealed in this study. This may be due to differences *in vitro* and *in vivo*, where the innate immune response against the virus may be more robust than in cell culture.

As shown in the present study, reverse genetics of HCV has become available for studies of HCV replication. The important factors for virus replication suggested above can be analysed further using this system.

We also examined the response of HCV-KT9-infected mice to IFN treatment. Three HCV-KT9-infected mice were treated with daily intramuscular injections of 1000 IU IFN- α (g body weight)⁻¹ for 2 weeks. This regimen resulted in a reduction in HCV RNA levels of only 1.0 log copies ml⁻¹ (data not shown). These results are consistent with our previous study, which showed a similar low-level reduction in HCV RNA in mice infected with a genotype 1a clone, and differ from our previous results in mice infected with HCV genotype 2a, which became negative for HCV RNA following daily treatment with 1000 IU IFN- α (g body weight)⁻¹ for 2 weeks (Hiraga *et al.*, 2007). These results are in agreement with our clinical experience that genotype 1 is more resistant to IFN therapy than genotype 2. As shown in the present study and previously (Hiraga *et al.*, 2007), reverse genetics of HCV with three genotypes, 1a, 1b and 2a, is now available. By recombination of these clones or the establishment of mutants with nucleotide and amino acid sequences similar to each other, it may be possible to clarify the mechanism underlying the variability in susceptibility of HCV genotypes to IFN.

In this study, HCV-KT9 showed no virus production ability *in vitro*. Recently, Kato *et al.* (2007) reported that the genotype 1b HCV clone CG1b replicated in Huh7.5.1 cells and produced infectious HCV. It will be of interest to create chimeric viruses of HCV-KT9 and HCV-CG1b, and to determine the mutations that are important for virus production *in vitro*.

In summary, we established an infection model of a genotype 1b HCV clone using human hepatocyte chimeric mice. This model will be useful for studies of HCV replication, particularly the mechanism underlying the variable resistance of HCV genotypes to IFN therapy.

ACKNOWLEDGEMENTS

The authors thank Rie Akiyama and Kana Kunihiro for their technical help and Dr Francis V. Chisari for providing the Huh7.5.1 cells. This work was supported in part by Grants-in-Aid for scientific research and development from the Ministry of Education, Sports, Culture and Technology and the Ministry of Health, Labor and Welfare, Japan.

REFERENCES

Beard, M. R., Abell, G., Honda, M., Carroll, A., Gartland, M., Clarke, B., Suzuki, K., Lanford, R., Sangar, D. V. & Lemon, S. M. (1999). An infectious molecular clone of a Japanese genotype 1b hepatitis C virus. *Hepatology* 30, 316–324.

Bukh, J., Pietschmann, T., Lohmann, V., Krieger, N., Faulk, K., Engle, R. E., Govindarajan, S., Shapiro, M., St Claire, M. & other authors (2002). Mutations that permit efficient replication of hepatitis C virus RNA in Huh-7 cells prevent productive replication in chimpanzees. *Proc Natl Acad Sci U S A* 99, 14416–14421.

Enomoto, N., Sakuma, I., Asahina, Y., Kurosaki, M., Murakami, T., Yamamoto, C., Ogura, Y., Izumi, N., Marumo, F. & other authors (1996). Mutations in the nonstructural protein 5A gene and response to interferon in patients with chronic hepatitis C virus 1b infection. *N Engl J Med* 334, 77–81.

Friebe, P. & Bartenschlager, R. (2002). Genetic analysis of sequences in the 3' untranslated region of hepatitis C virus that are important for RNA replication. *J Virol* 76, 5326–5338.

Fried, M. W., Shiffman, M. L., Reddy, K. R., Smith, C., Marinos, G., Goncales, F. L., Jr, Haussinger, D., Diago, M., Carosi, G. & other authors (2002). Peginterferon alfa-2a plus ribavirin for chronic hepatitis C virus infection. *N Engl J Med* 347, 975–982.

Gale, M. J., Jr, Korth, M. J., Tang, N. M., Tan, S. L., Hopkins, D. A., Dever, T. E., Polyak, S. J., Gretch, D. R. & Katze, M. G. (1997). Evidence that hepatitis C virus resistance to interferon is mediated through repression of the PKR protein kinase by the nonstructural 5A protein. *Virology* 230, 217–227.

Gojobori, T., Ishii, K. & Nei, M. (1982). Estimation of average number of nucleotide substitutions when the rate of substitution varies with nucleotide. *J Mol Evol* 18, 414–423.

Heller, T., Saito, S., Auerbach, J., Williams, T., Moreen, T. R., Jazwinski, A., Cruz, B., Jeurkar, N., Sapp, R. & other authors (2005). An *in vitro* model of hepatitis C virus production. *Proc Natl Acad Sci U S A* 102, 2579–2583.

Hiraga, N., Imamura, M., Tsuge, M., Noguchi, C., Takahashi, S., Iwao, E., Fujimoto, Y., Abe, H., Maekawa, T. & other authors (2007). Infection of human hepatocyte chimeric mouse with genetically

engineered hepatitis C virus and its susceptibility to interferon. *FEBS Lett* 581, 1983–1987.

Kato, T., Matsumura, T., Heller, T., Saito, S., Sapp, R. K., Murthy, K., Wakita, T. & Liang, T. J. (2007). Production of infectious hepatitis C virus of various genotypes in cell cultures. *J Virol* 81, 4405–4411.

Kneteman, N. M., Weiner, A. J., O'Connell, J., Collett, M., Gao, T., Aukerman, L., Kovalevsky, R., Ni, Z. J., Zhu, Q. & other authors (2006). Anti-HCV therapies in chimeric scid-Alb/uPA mice parallel outcomes in human clinical application. *Hepatology* 43, 1346–1353.

Lindenbach, B. D., Meuleman, P., Ploss, A., Vanwolleghem, T., Syder, A. J., McKeating, J. A., Lanford, R. E., Feinstone, S. M., Major, M. E. & other authors (2006). Cell culture-grown hepatitis C virus is infectious *in vivo* and can be recultured *in vitro*. *Proc Natl Acad Sci U S A* 103, 3805–3809.

Lohmann, V., Komer, F., Koch, J., Herian, U., Theilmann, L. & Bartenschlager, R. (1999). Replication of subgenomic hepatitis C virus RNAs in a hepatoma cell line. *Science* 285, 110–113.

Mercer, D. F., Schiller, D. E., Elliott, J. F., Douglas, D. N., Hao, C., Rinfret, A., Addison, W. R., Fischer, K. P., Churchill, T. A. & other authors (2001). Hepatitis C virus replication in mice with chimeric human livers. *Nat Med* 7, 927–933.

Okamoto, H., Kojima, M., Okada, S., Yoshizawa, H., Iizuka, H., Tanaka, T., Muchmore, E. E., Peterson, D. A., Ito, Y. & other authors (1992). Genetic drift of hepatitis C virus during an 8.2-year infection in a chimpanzee: variability and stability. *Virology* 190, 894–899.

Saitou, N. & Nei, M. (1987). The neighbor-joining method: a new method for reconstructing phylogenetic trees. *Mol Biol Evol* 4, 406–425.

Simmonds, P., Holmes, E. C., Cha, T. A., Chan, S. W., McOmish, F., Irvine, B., Beall, E., Yap, P. L., Kolberg, J. & other authors (1993). Classification of hepatitis C virus into six major genotypes and a series of subtypes by phylogenetic analysis of the NS-5 region. *J Gen Virol* 74, 2391–2399.

Takamizawa, A., Mori, C., Fuke, I., Manabe, S., Murakami, S., Fujita, J., Onishi, E., Andoh, T., Yoshida, I. & other authors (1991). Structure and organization of the hepatitis C virus genome isolated from human carriers. *J Virol* 65, 1105–1113.

Tateno, C., Yoshizane, Y., Saito, N., Kataoka, M., Utoh, R., Yamasaki, C., Tachibana, A., Soeno, Y., Asahina, K. & other authors (2004). Near completely humanized liver in mice shows human-type metabolic responses to drugs. *Am J Pathol* 165, 901–912.

Thomson, M., Nascimbeni, M., Gonzales, S., Murthy, K. K., Rehmann, B. & Liang, T. J. (2001). Emergence of a distinct pattern of viral mutations in chimpanzees infected with a homogeneous inoculum of hepatitis C virus. *Gastroenterology* 121, 1226–1233.

Tsuge, M., Hiraga, N., Takaishi, H., Noguchi, C., Oga, H., Imamura, M., Takahashi, S., Iwao, E., Fujimoto, Y. & other authors (2005). Infection of human hepatocyte chimeric mouse with genetically engineered hepatitis B virus. *Hepatology* 42, 1046–1054.

Wakita, T., Pietschmann, T., Kato, T., Date, T., Miyamoto, M., Zhao, Z., Murthy, K., Habermann, A., Krausslich, H. G. & other authors (2005). Production of infectious hepatitis C virus in tissue culture from a cloned viral genome. *Nat Med* 11, 791–796.

Yi, M. & Lemon, S. M. (2003). 3' Nontranslated RNA signals required for replication of hepatitis C virus RNA. *J Virol* 77, 3557–3568.

You, S. & Rice, C. M. (2008). 3' RNA elements in hepatitis C virus replication: kissing partners and long poly(U). *J Virol* 82, 184–195.

Zhong, J., Gastaminza, P., Cheng, G., Kapadia, S., Kato, T., Burton, D. R., Wieland, S. F., Uprichard, S. L., Wakita, T. & other authors (2005). Robust hepatitis C virus infection *in vitro*. *Proc Natl Acad Sci U S A* 102, 9294–9299.

Molecular Epidemiology and Interferon Susceptibility of the Natural Recombinant Hepatitis C Virus Strain RF1_2k/1b

Fuat Kurbanov,¹ Yasuhiro Tanaka,¹ Elena Chub,^{1,2} Isao Maruyama,² Aziza Azlarova,^{1,6} Hiroshi Kamitsukasa,⁴ Tomoyoshi Ohno,² Stefania Bonetto,⁷ Isabelle Moreau,¹ Liam J. Fanning,⁸ Florence Legrand-Abravanel,⁹ Jaques Izopet,⁸ Nikolai Naoumov,⁷ Takashi Shimada,³ Sergei Netesov,⁵ and Masashi Mizokami¹

¹Department of Clinical Molecular Informative Medicine, Nagoya City University Graduate School of Medical Sciences, and ²Department of Gastroenterology, Social Insurance, Chukyo Hospital, Nagoya, ³PhoenixBio, Hiroshima, and ⁴Department of Gastroenterology, Tokyo National Hospital, Tokyo, Japan; ⁵State Research Center of Virology and Biotechnology VECTOR Koltsovo, Novosibirsk Region, Russian Federation; ⁶Scientific Research Institute of Hematology and Blood Transfusion, Ministry of Health, Tashkent, Uzbekistan; ⁷Institute of Hepatology, 69–75 Chenies Mews, University College London, London, United Kingdom; ⁸Molecular Virology Diagnostic and Research Laboratory, Department of Medicine, Cork University Hospital/University College Cork, Cork, Republic of Ireland; and ⁹INSERM U563-IFR30 and Laboratoire de Virologie, Institut Fédératif de Biologie de Purpan, Toulouse, France

Background. Hepatitis C virus (HCV) genotype is an important determinant of virological response to antiviral therapies. Currently, there are no data available on the molecular epidemiology and interferon susceptibility of the natural intergenotypic recombinant RF1_2k/1b (RF1) strain.

Methods. Genotyping and RF1-PCR screening were performed on samples from 604 HCV RNA-positive individuals from 7 countries. uPA/SCID mice carrying human hepatocytes (chimeric mice) were infected with the RF1_2k/1b strain, and the susceptibility of the strain to interferon and ribavirin was compared with the susceptibilities of 2 different strains of genotype B, used as references.

Results. Six new RF1 cases were identified in this study; 5 (2%) of 281 in Russia and 1 (1%) of 90 in Uzbekistan. Phylogenetic analyses based on Core/E1 and NS5b indicated that all RF1 representatives share a common evolutionary ancestor. Infection with RF1 was established in chimeric mice. Reduction of RF1 viral load was observed in response to 3 injections of 3 μ g/kg pegylated-interferon alpha-2a alone or in combination with 50 mg/kg of ribavirin (0.5 or 1.4 log-copies/mL).

Conclusions. All identified RF1-type strains appear to be introduced from a single source, suggesting that intergenotypic recombination in HCV is sporadic and not associated with cocirculation of different genotypes in a population. The RF1 strain in this study was responsive to interferon *in vivo*.

Chronic infection with hepatitis C virus (HCV) is a leading cause of liver cirrhosis and hepatocellular carcinoma worldwide and is one of the major global public health problems. HCV strains isolated in different part of the world were classified into 6 genotypes (i.e., genotypes

1–6) and numerous subtypes (e.g., subtypes 1a and 1b) [1, 2]. Genotypes 1, 2, and 3 are widespread, whereas others are limited to certain areas [2]. Clinical studies have demonstrated that genotype is the strongest predictor of the virological response to interferon (IFN)-based therapy [3]. It is widely recognized that patients infected with genotype 2 in particular are more likely to achieve sustained virological response (SVR) than patients infected with genotype 1. Technically, HCV genotyping is usually based on a single genomic region, of

Received 19 November 2007; accepted 9 June 2008; electronically published 20 October 2008.

Potential conflicts of interest: none reported.

Financial support: Ministry of Health, Labour, and Welfare of Japan; Japan Society for the Promotion of Science; Viral Hepatitis Research Foundation of Japan (to F.K.).

Presented in part: 17th Conference of the Asian Pacific Association for the Study of the Liver, Kyoto, Japan, 27–30 March 2007; 58th Annual Meeting of the American Association for the Study of Liver Diseases, Boston, MA, 2–5 November.

The Journal of Infectious Diseases 2008; 198:1448–56

© 2008 by the Infectious Diseases Society of America. All rights reserved.
0022-1889/2008/19810-0006\$15.00
DOI: 10.1093/infdis/jin175

The nucleotide sequence data reported in this article will appear in the DDBJ/EMBL/GenBank nucleotide sequence databases (accession numbers AB327010-AB327059).

Reprints or correspondence: Dr. Masashi Mizokami, Dept. of Clinical Molecular Informative Medicine, Nagoya City University Graduate School of Medical Sciences, Kawasumi 1, Mizuho, Nagoya 467-8601, Japan (mizokami@med.nagoya-cu.ac.jp).

Table 1. Characteristics of the study population.

Risk factor	Country of origin, risk factor(s)								
	United Kingdom		Bulgaria	Lithuania	Russia	Uzbekistan	Mongolia	Japan	
	BT (n = 27)	IDU (n = 23)	IDU (n = 20)	BT (n = 9)	BT/IDU ^a (n = 281)	BT (n = 90)	BT (n = 67)	BT (n = 50)	IDU (n = 37)
Age, mean ± SD, years	45 ± 9	42 ± 7	23 ± 7	36 ± 16	29 ± 12	29 ± 14	53 ± 14	45 ± 10	46 ± 16
Male sex	14	19	13	6	175	73	25	27	27
Positive RF1 screening result	0	0	0	0	5 (2)	1 (1)	0	0	0
HCV genotype ^b									
1a	14 (52)	16 (70)	12 (60)	1 (11)	...	1 (1)
1b	8 (30)	3 (13)	2 (10)	4 (45)	153 (54)	44 (49)	67 (100)	28 (56)	...
2a	14 (5)	4 (5)	...	12 (24)	24 (66)
2b	10 (20)	6 (16)
2c	1 (11)	10 (4)
2k	1 (0.4)
3e	3 (11)	4 (17)	6 (30)	3 (33)	98 (35)	40 (44)
4	2 (7)

NOTE. Data are no. (%) of subjects, unless otherwise indicated. BT, blood transfusion and other medical-related procedures (e.g., injections, vaccination, surgery, and dental treatment); IDU, injection drug use.

^a BT was the risk factor for 173 (62%), IDU and iatrogenic exposures were risk factors for 30 (11%), and the risk factor was uncertain for 77 (27%). This latter cohort was not subdivided into IDU and BT.

^b Consensus of genotyping results for both Core/E1 and NS5B genes.

which 5'-UTR, Core/E1, or NS5B is most commonly used [2]. However, a series of recent studies have described natural intergenotypic recombinant forms of HCV that possess genotype 2 sequence in the structural parts of their genome and genotype 1, 5, or 6 in the nonstructural parts of their genome [4–8]. The first reports of these strains, designated RF1_2k/1b, were from Russia [4], Ireland [6], Estonia [9], and, most recently, Uzbekistan [10]. In present study, we applied Core/E1-based and NS5B-based genotyping, in addition to RF1_2k/1b screening, to assess the prevalence of recombinant HCV variants in different countries.

So far, no studies have been performed to define IFN susceptibility of intergenotypic recombinants. Mice with severe combined immunodeficiency, carrying urokinase-type plasminogen activator transgenes controlled by an albumin promoter (uPA/SCID), with the liver partially repopulated by human hepatocytes (chimeric mice) [11, 12], are, together with chimpanzees, the only widely recognized *in vivo* models to study HCV infection. It has previously been shown that chimeric mice infected with different HCV isolates can be treated with standard IFN and pegylated IFN [13]. In the present study, we use the chimeric mice to compare the *in vivo* susceptibility of the recombinant RF1 strain with that of resistant and susceptible representative strains of genotype 1b used as controls.

SUBJECTS, MATERIALS, AND METHODS

Study population. In total 604 anti-HCV-positive serum samples were obtained from the United Kingdom, Bulgaria,

Lithuania, Russia, Uzbekistan, Mongolia, and Japan during 2000–2006. The study was approved by institutional ethics committees at the respective study sites and was conducted in accordance with the Declaration of Helsinki. All specimens were obtained from treatment-naïve patients. Risk factors for HCV infection were assessed by direct interview, using a standardize protocol at the respective local clinical centers. Individuals were classified on the basis of risk factors, if known. The IDU group consisted of persons with a history of injection drug use and needle sharing, and the BT group consisted of persons with a history of blood transfusion, medical procedures (e.g., injections, vaccination, and surgery), or dental procedures. Table 1 summarizes the epidemiological data of the 604 serum donors split by the geographical origin.

Serological and molecular confirmation of the HCV infection. Total RNA was extracted using SepaGene RV-R (Sanko Junyaku). Complementary DNA was obtained using SuperScript II RNase H⁻ transcriptase (Invitrogen) and Random hexamer primer (Takara Shuzo). HCV RNA was quantified using a previously reported protocol with a detection threshold of ≥100 HCV copies/mL [14].

HCV genotyping. Structural (Core) and nonstructural (NS5B) viral genes were genotyped as described previously [15, 16].

HCV type RF1_2k/1b screening. Screening for the natural recombinant type RF1_2k/1b was performed using a method we designed to detect <10 genomic copies/assay (100 copies/mL) of the target sequence, even on a background of 10⁵ copies/assay of nonrecombinant template [10]. In brief, the primers targeting a

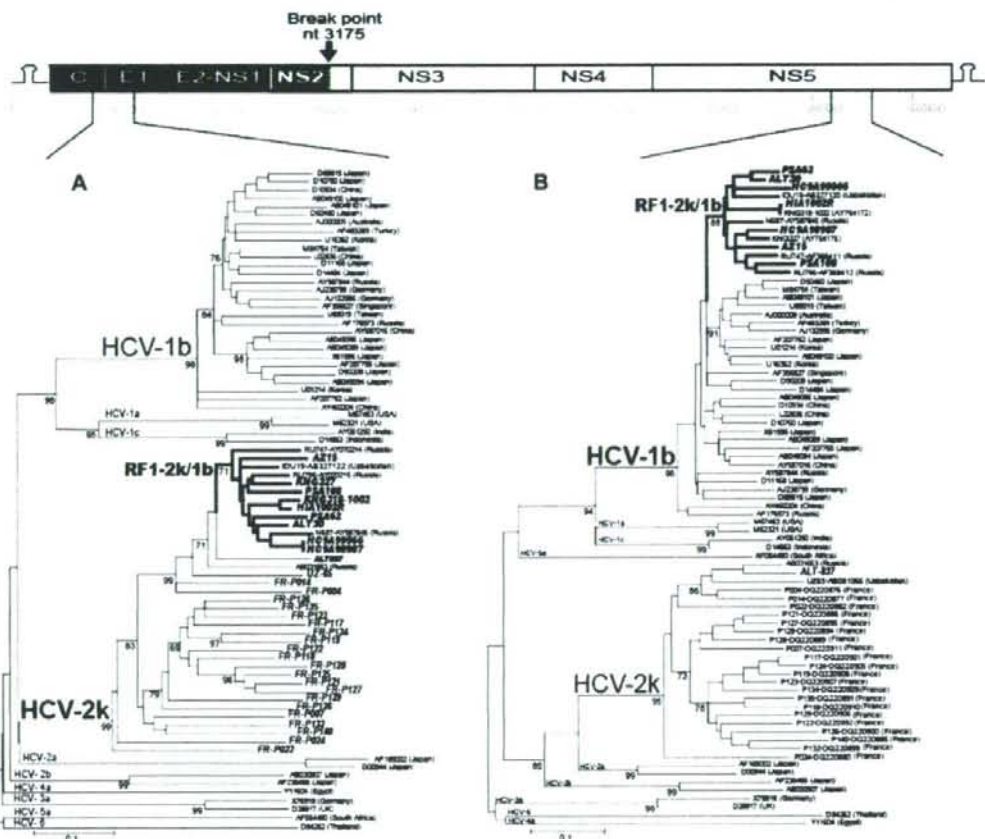


Figure 1. Phylogenetic relationship among hepatitis C virus (HCV) strains. The NJ tree was constructed on the basis of a 438-nucleic acid sequence of the Core/E1 coding region (nt 861–1298) (A) and 286 nt of the NS5B coding region (nt 8283–8568) (B). Position of the analyzed genomic parts is schematically demonstrated using HCV polyprotein coding map. A part of the RF1_2k/1b type HCV genome corresponding to HCV2k is shaded in *dark gray*, and the tentative break point is indicated by an *arrow*. Distances of the trees were estimated on basis of synonymous substitutions under a modified Nei-Gojobori model. Bootstrap resampling indexes exceeding 70% are indicated near to the roots of corresponding cluster. Strains sequenced in this study are indicated in *bold italic font*.

part of the NS2-coding region spanning the tentative intergenotypic break point specified for RF1_2k/1b (between nucleotides 2986 and 3270, according a reference HCV strain; Genbank accession number AF009606) [4].

Phylogenetic analyses. All specimens with positive results of RF1 screening were subjected to PCR amplification using pan-genotype primers for core/E1 (for nucleotides 859–1299) and NS5B (for nucleotides 8278–8618) genomic regions [17]. The PCR products were directly sequenced (Prism Big Dye [Applied Biosystems]) on the ABI 3100. Neighbor joining trees were constructed with Nei-Gojobori (synonymous substitutions p-distances) [18, 19].

Reference HCV-strains for phylogenetic analysis of the recombinant RF1_2k/1b strain. HCV complete genome sequences were retrieved from the DDBJ/EMBL/GenBank genetic

database and used as references in initial phylogenetic analyses of the recombinant strains identified in this study. To ensure that the reference sequences are both representative and maximally informative phylogenetically, a total of 30 geographically representative subtype 1b references were selected in random from serially reconstructed phylogenetic trees (figure 1). Partial NS5B sequences of 37 HCV-2k strains were available in the DDBJ/EMBL/GenBank genetic database from previous studies [10, 20]. For the present study, which used the above outlined primers for the E1/Core region, we sequenced 22 of 37 strains to be used in the phylogenetic analyses, along with the only complete genome reference of the HCV-2k [21] (figure 1). Core/E1 and NS5B sequences were also included for an HCV-2k strain found among Russian specimens in present study (table 1 and figure 1). A single complete-genome-reference of RF_2k/1b deposited in

Table 2. Characteristics of the 6 carriers of the RF1_2k/1b strain.

Carrier	Strain	Origin	Age, years	Sex	Risk factor	Clinical manifestation	Bilirubin level, $\mu\text{mol/L}^a$	ALT level, U/L ^b	AST level, U/L ^c
1	KNG-327	Russia	25	M	Unknown	IC	20	24	48
2	PSA-108	Russia	37	M	Unknown	IC	16	24	19
3	KNG-318	Russia	30	M	IDU	CH	20	78	42
4	PSA-62	Russia	50	M	BT	CH	12	43	25
5	ALT-30	Russia	34	F	Unknown	CH	15	87	72
6	AZ15	Uzbekistan	22	M	BT/IDU	CH	11	70	55

NOTE. ALT, alanine aminotransferase; AST, aspartate aminotransferase; BT, blood transfusion and other medical-related procedures (e.g., injections, vaccination, surgery, and dental treatment); CH, chronic hepatitis; F, female; IC, inactive carrier; IDU, injection drug use; M, male.

^a Normal range, 8.5–20.5 $\mu\text{mol/L}$.

^b Normal range, 8.0–40.0 U/L.

^c Normal range, 5.0–30.0 U/L.

the DDBJ/EMBL/GenBank genetic database (Genbank accession number: AY587845) [22] was available for the study, along with 3 partially sequenced strains [4, 10]. Two recombinant strains isolated from persons who emigrated from Russia to Ireland and for which 5' UTR, NS2, and NS5b regions were recently determined [6] were also subjected to sequencing and were included in the phylogenetic analysis (figure 1).

Selected reference strains were also included in the phylogenetic analysis to represent the following subtypes: HCV-1a, 1c, 2a, 2b, 3a, 4a, 5a, and 6 (figure 1).

Infection of chimeric mice and IFN susceptibility of the natural recombinant RF1_2k/1b strain. To investigate the ability of the RF1_2k/1b viral strain to establish infection and replication in mice, we used the previously described uPA/SCID mice with humanized liver [11]. The 9 mice used in the present study had received hepatocyte transplants from the same donor (a 10-year-old white girl). Transplantation of the hepatocytes, inoculation of virus, and administration of antiviral therapy were performed at PhoenixBio (Hiroshima, Japan), using protocols described previously [11]. Three mice were subjected to inoculation with serum obtained from an untreated RF1_2k/1b-infected carrier from Uzbekistan (ID:AZ-15) (table 2, figures 1 and 2). Two additional cohorts of 3 mice each were used as controls. Mice in the first cohort were inoculated with a serum sample obtained before therapy initiation from an HCV-1b-infected Japanese woman (age, 48 years) with fulminant hepatitis who had had sustained virological response to standard combination therapy (pegylated IFN plus ribavirin) (ID:SVR HCV-1b). Mice in the second cohort were inoculated with a serum sample obtained during treatment from an HCV-1b-infected Japanese man (age, 62 years) with chronic hepatitis who had had no response to standard treatment (ID:1b-NR). Both patients were treated and followed up during 2005–2006 at the Nagoya City University Hospital.

Each of the specimens described above was subjected to HCV quantification using RTD-PCR [14], and the exposure dose was

thereby standardized at $\sim 1.0 \times 10^5$ viral genome copies inoculated per mouse.

To test the susceptibility of the strains to pegylated IFN- α 2a (IFN), infected mice were treated with 3 injections (day 0, day 2 and day 5). Four protocols of the medication were modeled: monotherapy with IFN (Chugai) in doses of 3 $\mu\text{g}/\text{kg}$ (standard treatment dose), mono therapy with IFN (Chugai) in doses of 30 $\mu\text{g}/\text{kg}$ (10-fold treatment dose), monotherapy with ribavirin in doses of 10 mg/kg (standard clinical treatment dose) followed by 50 mg/kg (a 5-fold of the clinical treatment dose), and combined therapy with IFN (standard treatment dose) and ribavirin (5-fold treatment dose) (figure 3). HCV load was weekly measured in murine serum specimens.

Statistical analyses. Statistical differences were evaluated by the Fisher exact test or the χ^2 test with the Yates correction, using Stata, version 8.0 (StataCorp). Differences were considered significant if *P* values were $<.05$.

RESULTS

Detection of natural recombinant HCV strains in different populations. As shown in table 1, only 6 specimens were found to be positive by RF1 screening. Five specimens were from Russia, and one was from Uzbekistan. To confirm screening results, all 6 positive specimens were sequenced directly, using primers spanning tentative recombination break points in the NS2 coding region. Phylogenetic analysis indicated that these 6 strains along with 5 previously described RF1_2k/1b strains from Russia formed a tight cluster phylogenetically distinct from HCV-2k, HCV-1b, and other subtypes (figure 2). Visual inspection of the aligned sequences revealed the tentative recombination break point at nucleotide (nt) position 3175 in all of the strains formed the RF1_2k/1b cluster on the tree, which was consistent with previous publications (figure 2) [4, 6, 22].

Available epidemiological and clinical characteristics of the 6 carriers is summarized in table 2. Two of the individuals were asymptomatic, and the remaining 4 had biochemical markers

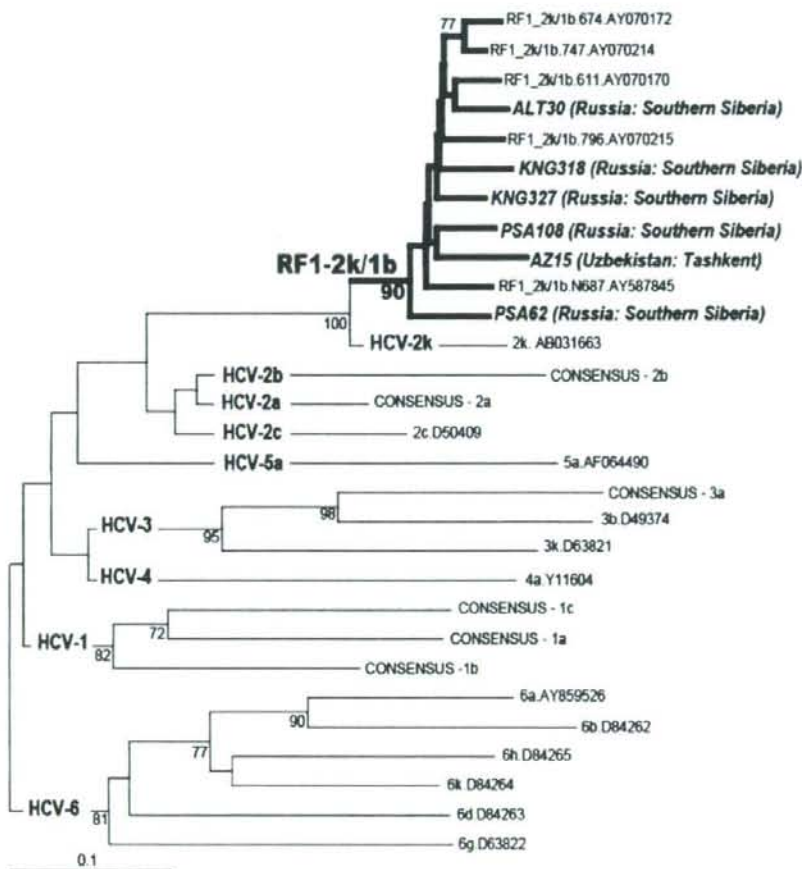


Figure 2. Phylogenetic affinity of hepatitis C virus (HCV) strains. The NJ tree was constructed on the basis of a 255-nucleic acid sequence of the NS2 coding region (nt 3015–3269). Distances corrected by Kimura (2-parameter method). Bootstrap resampling indexes exceeding 70% are indicated beneath the roots of the corresponding cluster. Six strains detected by RF1_2k/1b screening in this study are indicated in *bold italic font*, and the origin of the specimen is given in *parenthesis*. All of the HCV subtype reference sequences were retrieved from an on-line HCV database (available at: <http://hcv.lanl.gov/content/hcv-db/>). Subtype consensus sequences were used when available. The subtype and accession numbers are indicated. Strains sequenced in this study are indicated in *bold italic font*.

indicating chronic hepatitis (i.e., elevated alanine aminotransferase and aspartate aminotransferase levels).

To exclude possibility that other intergenotypic recombinants were present among the remaining 598 specimens, which had negative results of 2k/1b screening, these were subjected to genotyping in both structural (E1/Core) and nonstructural (NS5B) regions using genotype-specific primers. No genotype discordance was thereby observed between the structural and nonstructural genomic regions in all 598 cases. The genotyping results are summarized in table 1. In Russia and Uzbekistan, where the recombinant strain RF1 was detected, genotype 1b was the most prevalent, followed by genotype 3a. The nonrecombinant HCV-2k strain was detected in a minority of the Rus-

sian cohort and was not found among persons in the cohort from Uzbekistan (table 1).

Molecular evolutionary analyses of the recombinant strains. Phylogenetically, the recombinant strains isolated in the present study and those retrieved from the DDBJ/EMBL/GenBank genetic database were all tightly grouped together, forming a specific subcluster within the HCV-2k cluster on the Core/E1 tree (figure 1A) and within the HCV-1b cluster on the NS5B tree (figure 1B). The *t* score and bootstrap indexes estimated by MEGA (an interior branch test) were high but did not reach statistical significance (71% and 88% for the core/E1 and NS5B trees, respectively), possibly because of the short length of the sequence that was analyzed (figure 1). However, the phylogenetic affinity among all of

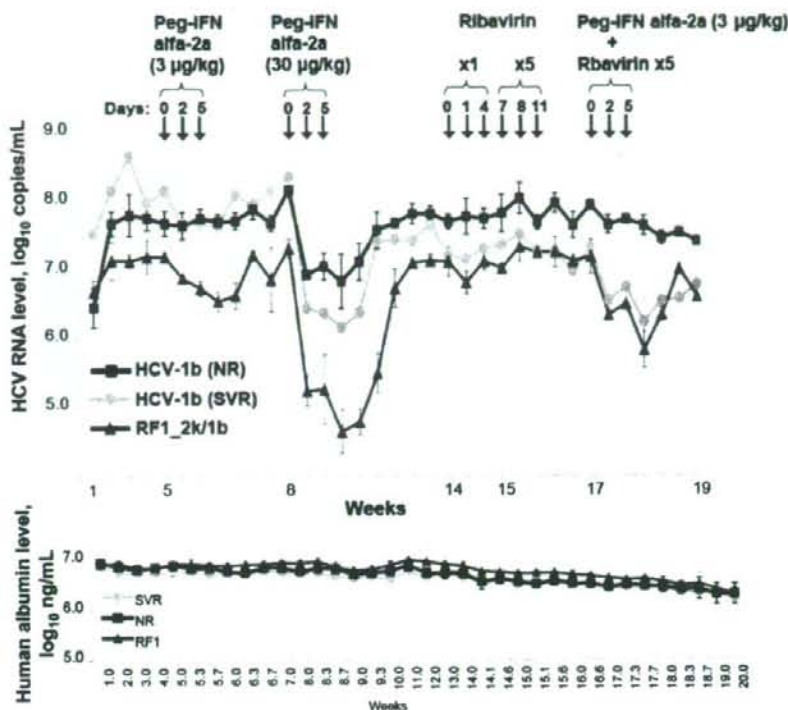


Figure 3. Time course studies in 9 mice inoculated with human serum samples positive for hepatitis C virus (HCV). RF1_2k/1b (AZ15, table 2), HCV-1b-NR (nonresponder reference) and HCV-1b-SVR (sustained virological responder reference) were intravenously injected into 3 mice each. HCV RNA titers (A) and concentrations of human serum albumin (B) measured in murine serum specimens. Mean HCV titers were calculated for each of the groups; SDs are indicated by vertical bars.

the RF1_2k/1b strains observed in 2 distant genomic regions indicates that the strains share single common ancestor.

In vivo infection of the HCV_2k/1b recombinant strain and susceptibility to IFN-based antiviral therapy. Three HCV strains were chosen as source inocula to confirm the ability of the RF1_2k/1b to infect chimeric mice and to determine the susceptibility of the strain to IFN treatment. The tentative IFN susceptibility determining region (ISDR) within the NS5A sequence [23] had been associated with HCV-1b susceptibility to IFN. The 3 strains were subjected to ISDR sequencing before inoculation in mice. Based on the original publication [23],

ISDR wild-type strains with sequences concordant with the reference HCV-J strain were considered to predispose strains to IFN resistance, whereas amino acid substitutions within the ISRD were considered to predispose strains to IFN susceptibility. The amino acid alignment versus the HCV-J reference strain is depicted in figure 4. The HCV isolated from the person with no response to IFN and ribavirin combination therapy was ISDR wild type, whereas the HCV-1b-SVR strain had 7 changes in the ISDR. The RF1_2k/1b strain (AZ-15) had a single amino acid change (from histidine to asparagine) at position 2218 and was therefore considered an intermediate type.



Figure 4. Amino acid sequence alignment of the part of the NS5A protein corresponding to residues 2138–2251 (relative to polyprotein start in H77) of hepatitis C virus (HCV) strains in 3 specimens used for inoculation to chimeric mice (specimens are the same as those in figure 3). Tentative interferon susceptibility determinant region (ISDR) [23] is indicated by the box. Amino acid residues are indicated by standard single-letter codes, and dots indicate residues identical to those in HCV-J, a reference strain (accession number D90208).

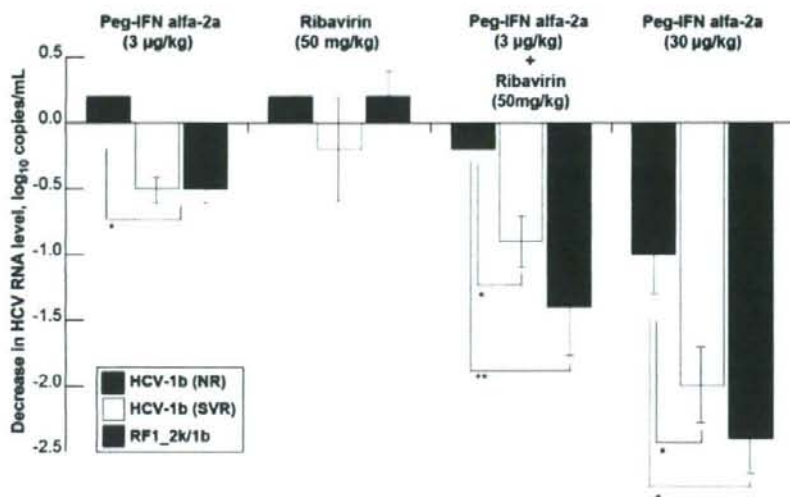


Figure 5. Reduction in hepatitis C virus (HCV) RNA titer observed on day 7 after treatment initiation. Mean reduction of the HCV RNA level from day 0 (baseline) was calculated for all 3 groups of mice; SDs are indicated by vertical bars. IFN, interferon.

By week 2 after inoculation of the infectious serum into chimeric mice, the mean HCV titers in the 1b-NR and RF1_2k/1b cohorts plateaued at around 7.6 and 7.0 log copies/mL, respectively. The 1b-SVR level increased to 8.5 log copies/mL until week 3 and then reached a plateau of ~8.0 log copies/mL (figure 3). These same animals were subsequently treated with 4 different regimens as outlined in materials and methods. Functionality of the human hepatocytes was estimated by measurement of human albumin levels in murine serum specimens (figure 3). The albumin levels were similar in the 3 groups, even though there was slight reduction of the albumin levels during the 19-week course of the experiment. At week 5 after inoculation, pegylated IFN- α -2a was administered in a dose of 3 μ g/kg. The mean decrease in the HCV RNA load was calculated for each of the 3 groups of mice, by comparison of the viral loads at day 0 (before the first injection) with that at day 7 (figure 5). No reduction of the HCV RNA titer was observed in the NR-1b group, whereas there was a reduction of 0.5 log copies/mL in the RF1_2k/1b and 1b-SVR groups ($P < .001$) (figure 5). Administration of the 10-fold dose of IFN (30 μ g/kg) induced 1.0, 2.0, and 2.4 log-copies/mL reductions in the HCV RNA titer for the 1b-NR, 1b-SVR, and RF1_2k/1b groups, respectively (figure 5). No significant difference was observed among the groups after administration of ribavirin in standard or 5-fold clinical doses (figure 3). Therefore, the 5-fold dose of ribavirin was further used in conjunction with the standard dose of IFN. Interestingly, after administration of the standard clinical dose of IFN in combination with the 5-fold dose of ribavirin, the viral load decreased by 1.4, 0.9, and 0.2 log-copies/mL in the RF1_2k/1b, SVR-1b, and NR-1b groups, respectively ($P < .02$) (figure 5).

The results indicated that, compared with controls, the RF1_2k/1b strain in this study was susceptible to IFN treatment, and high-dose pegylated IFN- α -2a (30 μ L/kg) monotherapy as well as standard dose pegylated IFN- α -2a (3 μ L/kg) in combination with ribavirin (50 mg/kg) led to a significant reduction of HCV RNA titers.

DISCUSSION

This study evaluated 2 important aspects of intergenotypic HCV recombination involving RF1_2k/1b: the epidemiology (distribution) and the susceptibility to IFN in an in vivo model. The former evaluation was accomplished using RF1_2k/1b-specific PCR screening and genotyping based on both structural and nonstructural genomic regions. HCV-infected samples from persons in 7 countries across Eurasia were used in this study.

One of the most important questions raised by all previous reports on HCV recombination involves the effect of recombination on the antiviral drug susceptibility of the strain [4–8, 22, 24, 25]. Furthermore, no data are available to date regarding the modeling of the natural intergenotypic recombinant HCV strains with respect to infection and replication in vivo. The present study is the first to indicate that the chimeric mouse model with human hepatocytes [11] is a relevant tool for investigation of the replication and antiviral susceptibility of the recombinant virus, particularly, RF1_2k/1b. The RF1_2k/1b is a hybrid of 2 distinct genotypes: genotype 2 can be effectively treated, whereas genotype 1 is difficult to treat. However, no data were available that characterized susceptibility of this type strain to antiviral treatment. The results of this investigation indicate

that the hybrid strain we studied exhibits susceptibility to pegylated IFN, and the observed viral kinetics were similar to those of SVR (another strain isolated from an HCV-1b-infected patient with fulminant hepatitis who eventually achieved sustained virological response and was used as an experimental reference in this study). In agreement with a previous study of so-called ISDR [23], NR strain (which was isolated from serum recovered from a nonresponding HCV-1b-infected patient during treatment and was used as a second reference in this study) had the IFN-resistant wild-type ISDR pattern, whereas the SVR strain had 7 mutations, classifying the strain as IFN-susceptible, ISDR-mutant type (figure 4). Interestingly, although the RF1_2k/1b strain in this study had a single mutation within the ISDR, it demonstrated IFN susceptibility that was slightly higher than that observed even for control 1b-SVR. This suggests that the NS5A ISDR pattern alone cannot explain the susceptibility of the strain in this case. Another genomic region possibly associated with response to IFN has been recently located in the core of HCV-1b, where amino acid substitutions at position 70 (from arginine to glutamine) and position 91 (from leucine to methionine) were identified as independent and significant factors associated with virological resistance to IFN [26]. In the present study, both NR and SVR strains, however, did not have the IFN-resistant substitutions, whereas the pattern of the recombinant strain corresponding to genotype 2k in this segment differed drastically in many positions. These results are concordant with conclusions of a clinical study recently performed in Europe, which stated that more complex interactions, with or without inclusion of the ISDR, likely exist and govern the HCV response to IFN treatment [27].

Using the PCR-screening assay for RF1_2k/1b detection [10], we detected 6 new strains in this study. The intergenotypic break point located for the strains corresponded to the nucleotide position 3175, which lies within the NS2 coding region, as was previously assessed in strains isolated from carriers in European part of Russia [4] and in persons who emigrated from Russia to Ireland [6]. Interestingly, in the present study we found 5 cases from the Asian part of Russia (specifically, southern Siberia) and 1 case in Uzbekistan, in addition to another case from Uzbekistan reported elsewhere [10]. No other cases were found among other cohorts. These cases might indicate that the variant is sporadically scattered within the countries of the former Soviet Union. However, further large-scale screening is required to confirm the global distribution of the strain.

To date, only 3 other reports, all based on complete or nearly complete HCV genome analysis, have described natural intergenotypic recombinant strains [5, 7, 8]. Interestingly, all of these reports concur with the initial report [4] with respect to the following observations: the intergenotypic break point is located between the structural and nonstructural genomic parts of HCV, within the NS2 coding region near the NS2/NS3 junction (nt 3175–3455); and all of

the recombinants had genotype 2 sequences (subtype 2b, 2i, and 2k) in the structural part of the genome.

None of the studied 598 cases (excluding RF1_2k/1b) had genotype discrepancies between the structural and nonstructural genomic regions. The HCV genotype distribution in each of the studied countries was similar to that previously reported from the United Kingdom [28], Lithuania [29], Russia [30], Uzbekistan [31], and Japan [15]. On one hand, this suggests that our cohorts provide a valid geographical representation for the studied countries, whereas on the other hand, this confirms that >1 genotype circulates in each of the regions (except Mongolia, where only 1b was detected). Nevertheless, no natural recombinant forms were detected other than RF1_2k/1b. These observations suggest that, unlike recombination in hepatitis B virus or HIV, recombination in HCV may not be associated with cocirculating genotypes. This also concurs with previous reports that have demonstrated rare dual-genotype coinfection among HCV-infected individuals [28, 32]. One possible explanation for this could be the superinfection exclusion phenomenon, depriving the viral strain of its translational and/or replication ability inside a cell that has been infected by another homologous virus. This was recently proven for HCV by delicate *in vitro* studies that used genotypes 1a, 1b, and 2a [33, 34]. Further experimental studies are required to confirm this hypothesis.

RF1_2k/1b virus was found only in Russia and Uzbekistan, where HCV-1b is highly prevalent. However, the prevalence of the nonrecombinant HCV-2k variant is exceptionally low in both countries. Furthermore, phylogenetic analyses of partial sequences in both structural and nonstructural genomic parts in this study indicated a specific phylogenetic clustering of the recombinant strains that was distinct from all nonrecombinant HCV-2k and HCV-1b reference strains in corresponding E1 and NS5B regions (figure 1A and 1B). Analysis by visual inspection of nucleotides and amino acid alignments in the NS2 region (data not shown) spanning the tentative recombination crossover point [4] revealed a high degree of similarity between all RF1 strains reported in this study and others [4, 6, 10]. This was also demonstrated by phylogenetic analysis based on a partial NS2 region (figure 2). Together, these observations strongly suggest that the current RF1_2k/1b viral population likely evolved from a single source introduction and subsequent spread rather than from a convergent evolution of distant strains. Based on the viral gene sequences and molecular clock principle, it is possible to estimate an approximate time of emergence of a common ancestor [35, 36]. When a previously estimated evolutionary rate [17] was applied to trace the evolution of all identified RF1 strains, the emergence of a recent common ancestor was dated between the 1930s and the 1960s (data not shown). These calculations concur with the approximate age of the HCV epidemics in the region [37, 38]. However, the number of the sequence strains available in this study was not large enough to obtain a statistically robust estimation of the ML.

In conclusion, this study demonstrates that natural HCV intergenotypic recombination is rare, sporadic, and not associated with cocirculation of different genotypes in a population. The RF1_2k/1b strain isolated in this study was susceptible to IFN. Further studies are required to confirm the epidemiological observations of this study and locate the genomic regions that contribute to IFN susceptibility.

Acknowledgments

We thank Dr. Marieta Simonova (Department of Gastroenterology, Military Hospital [Sofia, Bulgaria]) and Dr. Tsendsuren Oyunsuren (Laboratory of Molecular Biology, The Institute of Biology, Mongolian Academy of Sciences, Ulaanbaatar, Mongolia) for collecting serum samples used in this study.

References

1. Simmonds P, Bukh J, Combet C, et al. Consensus proposals for a unified system of nomenclature of hepatitis C virus genotypes. *Hepatology* 2005; 42:962–73.
2. Zein NN. Clinical significance of hepatitis C virus genotypes. *Clin Microbiol Rev* 2000; 13:223–35.
3. Scott JD, Gretch DR. Molecular diagnostics of hepatitis C virus infection: a systematic review. *JAMA* 2007; 297:724–32.
4. Kalinina O, Norder H, Mukomolov S, Magnius LO. A natural intergenotypic recombinant of hepatitis C virus identified in St. Petersburg. *J Virol* 2002; 76:4034–43.
5. Kageyama S, Agdamag DM, Alesna ET, et al. A natural intergenotypic (2b/1b) recombinant of hepatitis C virus in the Philippines. *J Med Virol* 2006; 78:1423–8.
6. Moreau I, Hegarty S, Levis J, et al. Serendipitous identification of natural intergenotypic recombinants of hepatitis C in Ireland. *Virology* 2006; 3:95.
7. Legrand-Abravanel F, Claudinon J, Nicot F, et al. New natural intergenotypic (2/5) recombinant of hepatitis C virus. *J Virol* 2007; 81:4357–62.
8. Noppornpanth S, Lien TX, Poovorawan Y, Smits SL, Osterhaus AD, Haagmans BL. Identification of a naturally occurring recombinant genotype 2/6 hepatitis C virus. *J Virol* 2006; 80:7569–77.
9. Tallo T, Norder H, Tefanova V, et al. Genetic characterization of hepatitis C virus strains in Estonia: fluctuations in the predominating subtype with time. *J Med Virol* 2007; 79:374–82.
10. Kurbanov F, Tanaka Y, Avazova D, et al. Detection of hepatitis C virus natural recombinant RF1_2k/1b strain among intravenous drug users in Uzbekistan. *Hepatology* 2007; 38:457–64.
11. Tateno C, Yoshizane Y, Saito N, et al. Near completely humanized liver in mice shows human-type metabolic responses to drugs. *Am J Pathol* 2004; 165:901–12.
12. Meuleman P, Libbrecht L, De Vos R, et al. Morphological and biochemical characterization of a human liver in a uPA-SCID mouse chimera. *Hepatology* 2005; 41:847–56.
13. Nakagawa S, Umehara T, Matsuda C, Kuge S, Sudoh M, Kohara M. Hsp90 inhibitors suppress HCV replication in replicon cells and humanized liver mice. *Biochem Biophys Res Commun* 2007; 353:882–8.
14. Takeuchi T, Katsume A, Tanaka T, et al. Real-time detection system for quantification of hepatitis C virus genome. *Gastroenterology* 1999; 116: 636–42.
15. Ohno O, Mizokami M, Wu RR, et al. New hepatitis C virus (HCV) genotyping system that allows for identification of HCV genotypes 1a, 1b, 2a, 2b, 3a, 3b, 4, 5a, and 6a. *J Clin Microbiol* 1997; 35:201–7.
16. Hashimoto M, Chayama K, Tubota A, et al. Typing six major hepatitis C virus genotypes by polymerase chain reaction using primers derived from nucleotide sequences of the NS5 region. *Int Hepatol Commun* 1996; 4:263–7.
17. Tanaka Y, Hanada K, Mizokami M, et al. A comparison of the molecular clock of hepatitis C virus in the United States and Japan predicts that hepatocellular carcinoma incidence in the United States will increase over the next two decades. *Proc Natl Acad Sci U S A* 2002; 99:15584–9.
18. Shin IT, Tanaka Y, Tateno Y, Mizokami M. Development and public release of a comprehensive hepatitis virus database. *Hepatology* 2008; 38:234–43.
19. Kuiken C, Mizokami M, Deleage G, et al. Hepatitis C databases, principles and utility to researchers. *Hepatology* 2006; 43:1157–65.
20. Thomas F, Nicot F, Sandres-Saune K, et al. Genetic diversity of HCV genotype 2 strains in south western France. *J Med Virol* 2007; 79:26–34.
21. Samokhvalov EI, Hijikata M, Gylka RI, Lvov DK, Mishiro S. Full-genome nucleotide sequence of a hepatitis C virus variant (isolate name VAT96) representing a new subtype within the genotype 2 (arbitrarily 2k). *Virus Genes* 2000; 20:183–7.
22. Kalinina O, Norder H, Magnius LO. Full-length open reading frame of a recombinant hepatitis C virus strain from St Petersburg: proposed mechanism for its formation. *J Gen Virol* 2004; 85:1853–7.
23. Enomoto N, Sakuma I, Asahina Y, et al. Mutations in the nonstructural protein 5A gene and response to interferon in patients with chronic hepatitis C virus 1b infection. *N Engl J Med* 1996; 334:77–81.
24. Colina R, Casane D, Vasquez S, et al. Evidence of intratypic recombination in natural populations of hepatitis C virus. *J Gen Virol* 2004; 85:31–7.
25. Moreno MP, Casane D, Lopez L, Cristina J. Evidence of recombination in quasispecies populations of a hepatitis C virus patient undergoing anti-viral therapy. *Virology* 2006; 3:87.
26. Akuta N, Suzuki F, Sezaki H, et al. Association of amino acid substitution pattern in core protein of hepatitis C virus genotype 1b high viral load and non-virological response to interferon-ribavirin combination therapy. *Intervirology* 2005; 48:372–80.
27. Torres-Puente M, Cuevas JM, Jimenez-Hernandez N, et al. Hepatitis C virus and the controversial role of the interferon sensitivity determining region in the response to interferon treatment. *J Med Virol* 2008; 80: 247–53.
28. Buckton AJ, Ngui SL, Arnold C, et al. Multitypic hepatitis C virus infection identified by real-time nucleotide sequencing of minority genotypes. *J Clin Microbiol* 2006; 44:2779–84.
29. Stikleryte A, Griskeviciene J, Magnius LO, Zagminas K, Norder H, Ambrozaitis A. Characterization of HCV strains in an oncohematological pediatric department reveals little horizontal transmission but multiple introductions by un-screened blood products in the past. *J Med Virol* 2006; 78:1411–22.
30. Shustov AV, Kochneva GV, Sivolobova GF, et al. Molecular epidemiology of the hepatitis C virus in Western Siberia. *J Med Virol* 2005; 77:382–9.
31. Kurbanov F, Tanaka Y, Sugauchi F, et al. Hepatitis C virus molecular epidemiology in Uzbekistan. *J Med Virol* 2003; 69:367–75.
32. Blackard JT, Sherman KE. Hepatitis C virus coinfection and superinfection. *J Infect Dis* 2007; 195:519–24.
33. Tschernie DM, Evans MJ, von Hahn T, et al. Superinfection exclusion in cells infected with hepatitis C virus. *J Virol* 2007; 81:3693–703.
34. Schaller T, Appel N, Koutsoudakis G, et al. Analysis of hepatitis C virus superinfection exclusion by using novel fluorochrome gene-tagged viral genomes. *J Virol* 2007; 81:4591–603.
35. Pybus OG, Rambaut A, Harvey PH. An integrated framework for the inference of viral population history from reconstructed genealogies. *Genetics* 2000; 155:1429–37.
36. Pybus OG, Charleston MA, Gupta S, Rambaut A, Holmes EC, Harvey PH. The epidemic behavior of the hepatitis C virus. *Science* 2001; 292: 2323–5.
37. Tanaka Y, Kurbanov F, Mano S, et al. Molecular tracing of the global hepatitis C virus epidemic predicts regional patterns of hepatocellular carcinoma mortality. *Gastroenterology* 2006; 130:703–14.
38. Nakano T, Lu L, Liu P, Pybus OG. Viral gene sequences reveal the variable history of hepatitis C virus infection among countries. *J Infect Dis* 2004; 190:1098–108.

Interaction of Hepatitis C Virus Nonstructural Protein 5A with Core Protein Is Critical for the Production of Infectious Virus Particles[▽]

Takahiro Masaki,¹ Ryosuke Suzuki,¹ Kyoko Murakami,¹ Hideki Aizaki,¹ Koji Ishii,¹ Asako Murayama,¹ Tomoko Date,¹ Yoshiharu Matsuura,² Tatsuo Miyamura,¹ Takaji Wakita,¹ and Tetsuro Suzuki^{1*}

Department of Virology II, National Institute of Infectious Diseases, Shinjuku-ku, Tokyo 162-8640, Japan,¹ and Department of Molecular Virology, Research Institute for Microbial Diseases, Osaka University, Suita-shi, Osaka 565-0871, Japan²

Received 17 April 2008/Accepted 22 May 2008

Nonstructural protein 5A (NS5A) of the hepatitis C virus (HCV) possesses multiple and diverse functions in RNA replication, interferon resistance, and viral pathogenesis. Recent studies suggest that NS5A is involved in the assembly and maturation of infectious viral particles; however, precisely how NS5A participates in virus production has not been fully elucidated. In the present study, we demonstrate that NS5A is a prerequisite for HCV particle production as a result of its interaction with the viral capsid protein (core protein). The efficiency of virus production correlated well with the levels of interaction between NS5A and the core protein. Alanine substitutions for the C-terminal serine cluster in domain III of NS5A (amino acids 2428, 2430, and 2433) impaired NS5A basal phosphorylation, leading to a marked decrease in NS5A-core interaction, disturbance of the subcellular localization of NS5A, and disruption of virion production. Replacing the same serine cluster with glutamic acid, which mimics the presence of phosphoserines, partially preserved the NS5A-core interaction and virion production, suggesting that phosphorylation of these serine residues is important for virion production. In addition, we found that the alanine substitutions in the serine cluster suppressed the association of the core protein with viral genome RNA, possibly resulting in the inhibition of nucleocapsid assembly. These results suggest that NS5A plays a key role in regulating the early phase of HCV particle formation by interacting with core protein and that its C-terminal serine cluster is a determinant of the NS5A-core interaction.

Hepatitis C virus (HCV) infection is a major public health problem and is prevalent in about 200 million people worldwide (27, 40, 42). Current protocols for treating HCV infection fail to produce a sustained virological response in as many as half of treated individuals, and many cases progress to chronic liver disease, including chronic hepatitis, cirrhosis, and hepatocellular carcinoma (15, 31, 35, 43).

HCV is a positive-strand RNA virus classified in the *Hepacivirus* genus within the *Flaviviridae* family (55). Its approximately 9.6-kb genome is translated into a single polypeptide of about 3,000 amino acids (aa), in which the structural proteins core, E1, and E2 reside in the N-terminal region. A crucial function of core protein is assembly of the viral nucleocapsid. The amino acid sequence of this protein is well conserved among different HCV strains compared to other HCV proteins. The nonstructural (NS) proteins NS3-NS5B are considered to assemble into a membrane-associated HCV RNA replicase complex. NS3 possesses the enzymatic activities of serine protease and RNA helicase, and NS4A serves as a cofactor for NS3 protease. NS4B plays a role in the remodeling of host cell membranes, probably to generate the site for the replicase assembly. NS5B functions as the RNA-dependent RNA polymerase. NS5A is known to play an important but undefined role in viral RNA replication.

NS5A is a phosphoprotein that can be found in basally phosphorylated (56 kDa) and hyperphosphorylated (58 kDa) forms (49). Comparative sequence analyses and limited proteolysis of recombinant NS5A have demonstrated that NS5A is composed of three domains (52). Domain I is relatively conserved among HCV genotypes compared to domains II and III. Analysis of the crystal structure of the conserved domain I that immediately follows the membrane-anchoring α -helix localized at the N terminus revealed a dimeric structure (53). The interface between protein molecules is characterized by a large, basic groove, which has been proposed as a site of RNA binding. In fact, its RNA binding property has been demonstrated biochemically (17). Domains II and III of NS5A are far less understood. Domain II contains a region referred to as the interferon sensitivity determining region, and this region and its C-terminal 26 residues have been shown to be essential for interaction with the interferon-induced, double-stranded RNA-dependent protein kinase (6–10, 38, 39, 48). Domain III includes a number of potential phosphoacceptor sites and is most likely involved in basal phosphorylation. This domain tolerates insertion of large heterologous sequences such as green fluorescent protein (GFP) and is not required for function of NS5A in HCV RNA replication (1, 34). However, a study with the recently established productive HCV cell culture system using genotype 2a isolate JFH-1 (28, 56, 58) demonstrated that while insertion of GFP within the NS5A region does not affect RNA replication, it does produce marked decreases in the production of infectious virus particles (41). This suggests that the C-terminal region of NS5A may affect virus particle production independent of RNA replication. Re-

* Corresponding author. Mailing address: Department of Virology II, National Institute of Infectious Diseases, 1-23-1 Toyama, Shinjuku-ku, Tokyo 162-8640, Japan. Phone: 81 3 5285 1111. Fax: 81 3 5285 1161. E-mail: tesuzuki@nih.go.jp.

[▽] Published ahead of print on 4 June 2008.

cently, Miyazaki et al. reported that the association of core protein with the NS proteins and replication complexes around lipid droplets (LDs) is critical for producing infectious viruses (33).

In the present study, we demonstrated that NSSA is a prerequisite for HCV particle production via its interaction with core protein, and we identified serine residues in the C-terminal region of NSSA that play an important role in virion production. Substitution of the serine residues with alanine residues inhibited not only the interaction of NSSA with core protein but also HCV RNA-core association and led to a decrease in HCV particle production with no effect on RNA replication.

MATERIALS AND METHODS

DNA construction. Plasmids pJFH1, which contains the full-length JFH-1 cDNA downstream of the T7 RNA promoter sequence, and pSGR-JFH1/Luc, in which the neomycin resistance gene of pSGR-JFH1 has been replaced by the firefly luciferase reporter gene, have been previously described (24, 56). To generate the fluorochrome gene-tagged full-length JFH-1 plasmid, pJFH1/NSSA-GFP, the region encompassing the RsrII site of NSSA and the BsrGI site of NSSB was amplified by PCR, the amplification product was cloned into pGEM-T Easy vector (Promega, Madison, WI), and the resultant plasmid was designated pGEM-JFH1/RsrII-BsrGI. A GFP reporter gene was amplified by PCR from pGreen Lantern-1 (Invitrogen, Carlsbad, CA) with primers containing the XhoI sequence and inserted, after restriction digestion with XhoI, into the XhoI site of pGEM-JFH1/RsrII-BsrGI. The resulting plasmid was digested by RsrII and BsrGI and ligated into pJFH1 similarly digested by RsrII and BsrGI to produce pJFH1/NSSA-GFP. For generation of the fluorochrome gene-tagged subgenomic reporter plasmid, pJFH1/NSSA-GFP was digested by RsrII and SnaBI and ligated into pSGR-JFH1/Luc similarly digested by RsrII and SnaBI. The mutations in the NSSA gene were generated by oligonucleotide-directed mutagenesis (57). To construct plasmids expressing N-terminally FLAG-tagged HCV core protein or hemagglutinin (HA)-tagged NSSA, DNA fragments encoding core protein or NSSA (wild type or mutants) were generated from the full-length JFH-1 cDNA by PCR. The core protein coding sequence, together with a FLAG sequence linked to its N terminus, was cloned into the pCAGGS vector (37). The coding sequences of NSSA, together with an HA sequence linked to their N termini, were also cloned into pCAGGS vectors. All PCR products were confirmed by automated nucleotide sequencing with an ABI Prism 3130 Avant Genetic Analyzer (Applied Biosystems, Tokyo, Japan).

Cells and viruses. The human hepatoma cell line, Huh-7, and JFH1/4-1 cells, which are Huh-7 cells carrying a subgenomic replicon of JFH-1 (32), were maintained in Dulbecco's modified Eagle's medium (DMEM) supplemented with minimal essential medium nonessential amino acids (Invitrogen), 100 units/ml penicillin, 100 µg/ml streptomycin, and 10% fetal bovine serum (FBS) at 37°C in a 5% CO₂ incubator. Huh-7-p7 cells, which are Huh-7 cells stably expressing the proteins core to p7 derived from the JFH-1 strain (18), were incubated in DMEM containing 300 µg/ml of zeocin (Invitrogen). HCV particles derived from JFH-1 were produced by transient transfection of Huh-7 cells with *in vitro* transcribed RNA, as described previously (56, 58). Recombinant vaccinia virus strain DIs, which expresses the bacteriophage T7 RNA polymerase under the control of the vaccinia virus early/late promoter P7.5, was generated and propagated as previously described (19).

DNA transfection, immunoprecipitation (IP), and immunoblotting. For co-expression of FLAG-tagged core protein and HA-tagged NSSA, cells were seeded onto 35-mm wells of a six-well cell culture plate and cultured overnight. Plasmid DNAs (2 µg) were transfected into cells using TransIT-LT1 transfection reagent (Mirus, Madison, WI). Cells were harvested at 48 h posttransfection, washed three times with 1 ml of ice-cold phosphate-buffered saline (PBS), and suspended in 0.25 ml lysis buffer (20 mM Tris-HCl [pH 7.4] containing 135 mM NaCl, 1% Triton X-100, 0.05% sodium dodecyl sulfate [SDS], and 10% glycerol) supplemented with 50 mM NaF, 5 mM Na₂VO₄, 1 µg/ml leupeptin, and 1 mM phenylmethylsulfonyl fluoride (PMSF). Cell lysates were sonicated at 4°C for 5 min, incubated for 30 min at 4°C, and centrifuged at 14,000 × g for 5 min at 4°C. After preclearing, the supernatant was immunoprecipitated with 10 µl of anti-FLAG M2-agarose beads (Sigma, St. Louis, MO). For expression of the full-length HCV polyprotein, Huh-7 cells transfected with 10 µg of *in vitro* transcribed RNAs by electroporation were resuspended in 20 or 30 ml of culture

medium, and 10-ml aliquots were seeded into 100-mm culture dishes. At 72 h posttransfection, the cells were incubated in 0.5 ml of lysis buffer (20 mM Tris-HCl [pH 7.4] containing 135 mM NaCl, 1% Triton X-100, 0.5% sodium deoxycholate, and 10% glycerol) supplemented with 50 mM NaF, 5 mM Na₂VO₄, 1 µg/ml leupeptin, and 1 mM PMSF. After preclearing, the supernatant was immunoprecipitated with 5 µg of polyclonal anti-NSSA antibody (34a) or polyclonal anti-C/EBPβ antibody (Santa Cruz Biotechnology, Santa Cruz, CA), and 20 µl of protein G-agarose beads (Invitrogen). The immunocomplex was precipitated with the beads by centrifugation at 800 × g for 30 s and then washed five times with lysis buffer by centrifugation. The proteins binding to the beads were boiled in 20 µl of SDS sample buffer and then subjected to SDS-12.5% polyacrylamide gel electrophoresis (PAGE). The proteins were transferred onto a polyvinylidene difluoride membrane (Immobilion; Millipore, Bedford, MA) and then reacted with a primary antibody and a secondary horseradish peroxidase-conjugated antibody. The immunocomplexes were visualized with an ECL Plus Western Blotting Detection System (GE Healthcare, Buckinghamshire, United Kingdom) and detected using an LAS-3000 imaging analyzer (Fujifilm, Tokyo, Japan).

***In vitro* synthesis of HCV RNA and RNA transfection.** Plasmid DNAs were digested with XbaI and treated with mung bean nuclease (New England Biolabs, Ipswich, MA) to remove the four terminal nucleotides, resulting in the correct 3' end of the HCV cDNA. Digested DNAs were purified and used as templates for RNA synthesis. HCV RNA was synthesized *in vitro* using a MEGAScript T7 kit (Ambion, Austin, TX). Synthesized RNA was treated with DNase I (Ambion), followed by acid guanidinium thiocyanate-phenol-chloroform extraction to remove any remaining template DNA. Synthesized HCV RNAs were used for electroporation. Trypsinized Huh-7 cells were washed with Opti-MEM I reduced-serum medium (Invitrogen) and resuspended at 3 × 10⁶ cells/ml with Cytomix buffer (54). RNA was mixed with 400 µl of cell suspension and transferred into an electroporation cuvette (Precision Universal Cuvettes; Thermo Hybaid, Middlesex, United Kingdom). Cells were then pulsed at 260 V and 950 µF using a Gene Pulser II unit (Bio-Rad, Hercules, CA). Transfected cells were immediately transferred onto six-well culture plates or 100-mm culture dishes.

Luciferase assay. Cells were harvested at different time points posttransfection of subgenomic reporter replicons and lysed in passive lysis buffer (Promega). The luciferase activity in cells was determined using a luciferase assay system (Promega).

Quantification of HCV core protein. HCV core protein in transfected cells or cell culture supernatants was quantified using a highly sensitive enzyme immunoassay (Ortho HCV antigen ELISA Kit; Ortho Clinical Diagnostics, Tokyo, Japan). To determine intracellular core protein amounts, cell lysates were prepared as described previously (41). To determine the efficiency of core protein release, the ratio of extracellular core protein to total core protein (the sum of intra- and extracellular core protein amounts) was calculated.

Intra- and extracellular infectivity assay. Culture supernatants were harvested 72 h posttransfection, and virus titers were determined by a 50% tissue culture infectious dose (TCID₅₀) assay as described previously (28, 46). Virus titration was performed by seeding naive Huh-7 cells in 96-well plates at a density of 1 × 10⁴ cells/well. Samples were serially diluted fivefold in complete growth medium and used to infect the seeded cells (six wells per dilution). At 72 h after infection, the inoculated cells were fixed and immunostained with a mouse monoclonal anti-core protein antibody (2H9) (56), followed by an Alexa Fluor 488-conjugated anti-mouse immunoglobulin G (IgG) (Invitrogen). Wells that showed at least one core protein-expressing cell was counted as positive. Cell-associated infectivity was determined essentially as described previously (12, 47). Briefly, cells were extensively washed with PBS, scraped, and centrifuged for 3 min at 120 × g. Cell pellets were resuspended in 1 ml of DMEM containing 10% FBS and subjected to four cycles of freezing and thawing using dry ice and a 37°C water bath. Samples were then centrifuged at 2,400 × g for 10 min at 4°C to remove cell debris, and cell-associated infectivity was determined by TCID₅₀ assay.

Expression of HCV proteins using vaccinia viruses, metabolic labeling of cells, and radioimmunoprecipitation analysis. Metabolic labeling of cells and radioimmunoprecipitation analysis were performed as described by Huang et al. (17) with some modifications. A total of 4 × 10⁶ Huh-7 cells were seeded onto each well of six-well cell culture plates and cultured overnight. A 2-µg amount of subgenomic replicon DNAs carrying defined NSSA mutations was transfected into cells using TransIT-LT1 transfection reagent, and at 12 h posttransfection the cells were then infected at a multiplicity of infection of 10 with recombinant vaccinia viruses expressing the T7 RNA polymerase. After 40 h of transfection, cells were incubated in methionine- and cysteine-deficient DMEM (Invitrogen) or phosphate-deficient DMEM (Invitrogen) for 2 h and labeled for 6 h with [³⁵S]methionine and [³⁵S]cysteine (200 µCi/well; GE Healthcare) or

[32 P]orthophosphate (250 μ Ci/well; GE Healthcare). The cells were then washed twice with cold PBS and lysed with SDS lysis buffer (50 mM Tris-HCl [pH 7.6], 0.5% SDS, 1 mM EDTA, 20 μ M PMSF). The cell lysates were passed through a 27-gauge needle several times to shear cellular DNA. After a 10-min incubation at 75°C, the lysates were clarified by centrifugation and diluted five-fold with HNAET buffer (50 mM HEPES [pH 7.5], 150 mM NaCl, 0.67% bovine serum albumin, 1 mM EDTA, 0.33% Triton X-100). After preclearing by incubation with 20 μ l of protein G-agarose beads for 1 h at 4°C, the supernatant was incubated with 2 μ l of rabbit polyclonal anti-N5SA antibody overnight at 4°C. A 20- μ l aliquot of protein G-agarose beads was further added and incubated for 2 h at 4°C. The cell pellets were washed three times with 0.5 ml of HNAETS buffer (HNAET containing 0.5% SDS), followed by washing once with 0.5 ml of HNE buffer (50 mM HEPES [pH 7.5], 150 mM NaCl and 1 mM EDTA). After treatment with or without λ protein phosphatase (New England Biolabs), the cell pellets were suspended in 20 μ l of SDS sample buffer and boiled for 10 min. The proteins were resolved on 10% SDS-polyacrylamide gels and analyzed by autoradiography.

Subcellular fractionation analysis. All steps were carried out at 4°C in the presence of a protease inhibitor cocktail (Complete; Roche, Mannheim, Germany) as described previously (20), with some modifications. Cells were suspended in four cell volumes of homogenization buffer (50 mM NaCl, 10 mM triethylamine [pH 7.4], 1 mM EDTA), snap frozen in liquid nitrogen, stored at -80°C, and thawed in a water bath at room temperature. Supernatants (0.4 ml) were layered on linear 10-ml iodixanol gradients from 2.5 to 25% and centrifuged at 37,000 rpm for 3.5 h in an SW41 rotor (Beckman, Fullerton, CA), followed by collection of 0.8-ml fractions from the top. Each fraction was concentrated by Centricon YM30 (Millipore), separated by SDS-PAGE, and immunoblotted with a rabbit polyclonal anti-calnexin antibody (Stressgen Biotechnologies, Victoria, Canada), a mouse monoclonal anti-adipose differentiation-related protein (ADRP) antibody (Progen Biotechnik, Heidelberg, Germany), or a rabbit polyclonal anti-N5SA antibody. The core protein amount in each fraction was also determined by enzyme-linked immunosorbent assay (ELISA).

IP-RT-PCR. The process of cell lysis to RNA purification was carried out as described by Johnson et al. (21) with some modifications. A total of 3×10^6 Huh-7 cells were transfected with 10 μ g of in vitro transcribed HCV RNAs and resuspended in 20 or 30 ml of culture medium, after which 10-ml aliquots were seeded into 100-mm culture dishes. At 72 h posttransfection, the cells were scraped and incubated in 500 μ l of hypotonic buffer (10 mM HEPES [pH 7.6], 1.5 mM MgCl₂, 10 mM KCl, 0.2 mM PMSF) per dish. The cells were passed through a 20-gauge needle several times, lysed with Nonidet P-40 at a final concentration of 1%, and incubated on ice for an additional 10 min. After centrifugation at 4,000 \times g at 4°C for 15 min, glycerol was added to the supernatants at a final concentration of 5%. The cell lysates were incubated with 20 μ l of protein G-agarose beads for 30 min at room temperature. After the cell lysates were removed from protein G-agarose beads, 5 μ g of mouse monoclonal anti-core protein antibody or normal mouse IgG (Sigma) as a negative control was added, and samples were incubated for an additional 1 h at room temperature. A 20- μ l aliquot of protein G-agarose beads per sample was added to the cell lysates and incubated for 1 h. After incubation, the beads were washed three times with wash buffer (10 mM Tris-HCl [pH 7.6], 100 mM KCl, 5 mM MgCl₂, and 1 mM dithiothreitol) and eluted in 100 μ l of elution buffer (50 mM Tris-HCl [pH 8.0], 1% SDS, and 10 mM EDTA) at 65°C for 10 min. After treatment with 100 μ g of proteinase K at 37°C for 30 min, the RNAs in immunocomplexes were isolated by acid guanidinium thiocyanate-phenol-chloroform extraction. Reverse transcriptase PCR (RT-PCR) was carried out using random hexamer and Superscript II RT (Invitrogen), followed by nested PCR with LA *Taq* DNA polymerase (TaKaRa, Shiga, Japan) and primer sets amplifying the fragments of nucleotides (nt) 129 to 2367 and nt 7267 to 9463 of the JFH-1 genome. To amplify the fragment of nt 129 to 2367, the sense primer 5'-CTGTGAGGAAC TACTGTCTT-3' and the antisense primer 5'-TCCACGATGTTCTGGTGAAG-3' were used for first-round PCR; the sense primer 5'-CGGGAGAGCCAT AGTGG-3' and the antisense primer 5'-CATTCCGTGGTAGAGTGCA-3' were used for second-round PCR. To amplify the fragment of nt 7267 to 9463, the sense primer 5'-GTCCAGGGTCCCGTCTGGACT-3' and the antisense primer 5'-GCGGCTCAGGACCTTTCAC-3' were used for first-round PCR; the sense primer 5'-CACCGTGTGGTGTGGTCT-3' and the antisense primer 5'-GTGTACTAGTGTGGCGTCTCA-3' were used for second-round PCR.

Indirect immunofluorescence analysis. Cells incubated for 3 days after transfection with JFH-1 RNAs were seeded in an eight-well chamber slide (BD Biosciences, San Jose, CA) and cultured overnight. The adherent cells were washed twice with PBS and fixed with 4% paraformaldehyde at room temperature. After a washing step with PBS, the cells were permeabilized with PBS containing 0.3% Triton X-100 and 2% FBS for 1 h at room temperature and

stained with a rabbit polyclonal anti-N5SA antibody and a mouse monoclonal anti-core protein antibody. The fluorescent secondary antibodies were Alexa Fluor 488- or Alexa Fluor 555-conjugated anti-rabbit or anti-mouse IgG antibodies (Invitrogen). Analyses of JFH-1 were performed on a Zeiss confocal laser scanning microscope LSM 510 (Carl Zeiss, Oberkochen, Germany).

RESULTS

Mutations of serine residues at the N5SA C terminus impair basal phosphorylation but have little effect on viral RNA replication. As demonstrated in a previous study, insertion of GFP into the N5SA C terminus does not significantly affect viral RNA replication but reduces the generation of infectious HCV particles (41). The C-terminal region of N5SA contains highly conserved serine residues that are involved in basal phosphorylation (1, 23, 49). To examine the involvement of the serine clusters (cluster 3-A [CL3A] and cluster 3-B [CL3B]) in the C-terminal region of N5SA in HCV particle production, we created mutated HCV genomes as well as subgenomic replicons carrying alanine substitutions for the conserved serine residues at aa 2384, 2388, 2390, and 2391 (residues are numbered according to the positions within the original JFH-1 polyprotein) (CL3A/SA); at aa 2428, 2430, and 2433 (CL3B/SA); or an in-frame deletion spanning aa 2384 to 2433 (Δ 2384-2433) (Fig. 1). A construct with an in-frame insertion of GFP (N5SA-GFP) was also generated as described previously for the Con1 isolate (34).

First, we analyzed the effects of the N5SA mutations on HCV RNA replication using a transient RNA replication assay using subgenomic luciferase reporter replicons (Fig. 2A) and found that the serine-to-alanine substitutions (CL3A/SA and CL3B/SA) did not affect viral RNA replication. N5SA-GFP and Δ 2384-2433 slightly reduced RNA replication, indicating that the mutations of the N5SA C terminus tested in this study do not critically affect RNA replication, which is consistent with previous reports (1, 34, 51).

Next, the phosphorylation status of the mutated N5SA was analyzed as described in Materials and Methods (Fig. 2B). N5SA was isolated from radiolabeled cells by IP and analyzed either directly by SDS-PAGE or after treatment with λ protein phosphatase. Analysis of 32 P-radiolabeled proteins revealed that the CL3A/SA, CL3B/SA, and Δ 2384-2433 mutations resulted in marked reduction of basal phosphorylation (Fig. 2B, compare lane 1 with lanes 3, 5, and 7 in the top panel). All 32 P-labeled N5SA proteins were sensitive to treatment with phosphatase (lanes 2, 4, 6, and 8). The possibility that loss of signal after dephosphorylation was due to contaminating proteases present in the phosphatase preparations can be ruled out because no degradation of the 35 S-labeled proteins was observed (Fig. 2B, bottom panel). These results suggest that mutations in the C-terminal serine cluster of N5SA impair basal phosphorylation but have no significant effect on viral RNA replication.

Effect of mutations introduced into the N5SA C terminus on the production of infectious HCV particles. To analyze HCV particle production from cells transfected with the in vitro transcribed viral genomic RNAs, we harvested supernatants and cells at 4, 24, 48, 72, and 96 h posttransfection and measured the amounts of core protein. As shown in Fig. 3A, comparable amounts of core proteins were detected in all transfected cells 4 h after transfection, reflecting unchanged

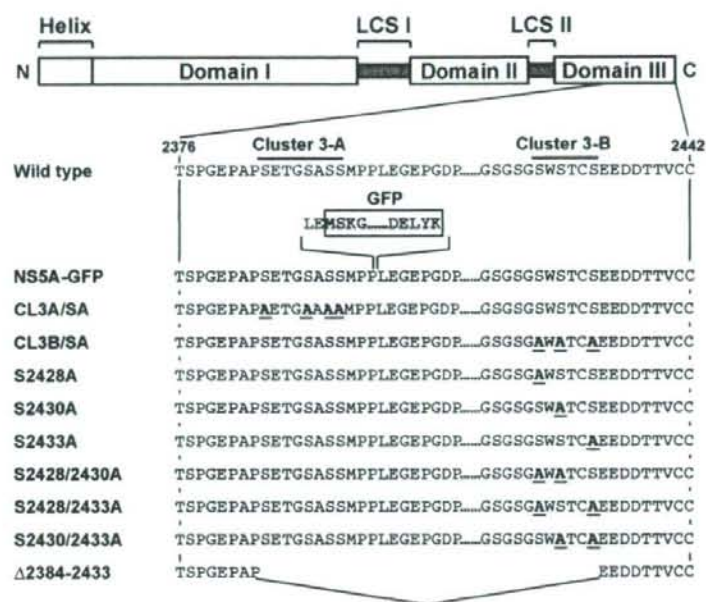


FIG. 1. Structures of HCV constructs used in this study. Schematic diagram of the NSSA structure according to Tellinghuisen et al. (52) is shown in the top panel. The three domains are indicated by white boxes and are separated by trypsin-sensitive regions with presumably low structural complexity (low-complexity sequence [LCS]). The numbers indicate amino acid residues within the original JFH-1 polyprotein. The names listed on the left represent full-length HCV constructs, subgenomic reporter replicons, or N-terminally HA-tagged NSSA constructs used in this study. NSSA-GFP carries a GFP insertion between aa 2394 and 2395 as indicated by a shaded box. CL3A/SA and CL3B/SA carry several serine-to-alanine substitutions in the NSSA C terminus constructed as described previously (1). HCV constructs from S2428A to S2430/2433A carry single or double serine-to-alanine substitutions generated by modification of the CL3B/SA construct. The Δ2384-2433 mutant possesses an in-frame deletion in the C-terminal region of NSSA. Amino acid substitutions are marked in bold and underlined. N and C represent N terminus and C terminus, respectively.

transfection efficiencies, and the kinetics of intracellular core protein levels was similar among transfectants. By contrast, core protein released from cells transfected either with the mutated genome of CL3B/SA, Δ2384-2433, or NSSA-GFP was more than 10-fold lower than that for the wild-type JFH-1 or CL3A/SA (Fig. 3B). Figure 3C shows the efficiency of core protein release from each transfectant, which is expressed as a percentage of the extracellular core protein level relative to the amount of total core protein (the sum of intra- and extracellular core protein). Core protein release efficiency with the wild type and CL3A/SA was 2 to 13% at 48 to 96 h after transfection, while only 1% or less of core protein was released in the cases of CL3B/SA, Δ2384-2433, and NSSA-GFP strains.

To further investigate production and release of infectious virus particles, naive Huh-7 cells were infected with culture supernatants of cells harvested 72 h posttransfection, and infectious virus titers were determined by TCID₅₀ assay at 72 h after infection. Figure 3D shows that release of infectious virus particles from cells transfected with the genome of CL3B/SA or Δ2384-2433 mutants was markedly reduced (about 10,000-fold) compared to that from wild-type- or CL3A/SA-transfected cells (white bars). To examine whether such a decrease in infectious HCV in the culture supernatants was attributable to defective virion assembly or impaired release of virions, we determined cell-associated infectivity (Fig. 3D). Production of

intracellular infectious virions in CL3B/SA- and Δ2384-2433-transfected cells was strongly impaired in comparison with that in wild-type-transfected (~1,000-fold) and CL3A/SA-transfected (~100-fold) cells. Thus, the results suggest a potential role for the serine cluster at aa 2428, 2430, and 2433 of NSSA in assembly of infectious HCV particles. Among the NSSA mutations tested, CL3B/SA is of particular interest because this mutation leads to a marked reduction in HCV production with no impact on viral RNA replication.

Serine residues at aa 2428, 2430, and 2433 are important for the interaction between NSSA and core protein. Miyazaki et al. reported that the association of core protein with NS proteins is critical for infectious HCV production and that mutations of the core protein and NSSA that cause these proteins to fail to associate with each other impair the production of infectious virus (33). Based on these observations and the findings noted above, we hypothesize that NSSA plays a key role in recruiting viral RNA, which is synthesized at the viral replication complex, to nucleocapsid formation via interaction between the NSSA C-terminal region and the core protein. To prove this, we analyzed the interaction of NSSA with the core protein by coimmunoprecipitation experiments. HA-tagged NSSA constructs carrying defined mutations were generated (Fig. 1) and coexpressed with the FLAG-tagged core protein in Huh-7 cells. As shown in Fig. 4A, coimmunoprecipitation of NSSA

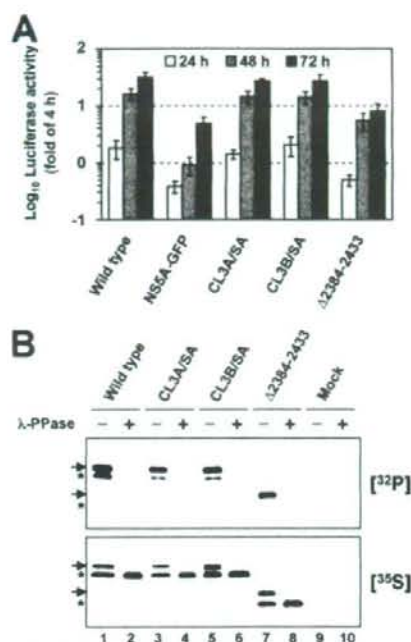


FIG. 2. Mutations at the C terminus of NS5A impair basal phosphorylation and have only a minor impact on RNA replication. (A) Replication of given mutants in transfected Huh-7 cells as determined by luciferase reporter assays performed at 24, 48, and 72 h posttransfection (white, gray, and black bars, respectively). Values given were normalized for transfection efficiency using the luciferase activity determined 4 h after transfection, which was set to 1. Mean values of quadruplicate measurements and the standard deviations are given. (B) Phosphorylation analysis of NS5A using the vaccinia virus T7 hybrid system. NS3-to-NS5B polyprotein fragments carrying the mutations specified above the lanes were transfected into Huh-7 cells, and proteins were radiolabeled with [³²P]orthophosphate or [³⁵S]methionine and [³⁵S]cysteine. NS5A proteins were isolated by IP and separated by SDS-PAGE (10% polyacrylamide). Mock-transfected cells served as a negative control (lanes 9 and 10). Half of the samples were treated with λ protein phosphatase (λ-PPase) (+) whereas the other half was mock treated (-) prior to SDS-PAGE. Arrows and asterisks indicate hyperphosphorylated and basally phosphorylated forms, respectively.

with the core protein was observed in cells expressing the wild-type NS5A and the CL3A/SA-mutated NS5A, but the amount of immunoprecipitated NS5A in the CL3A/SA-expressing cells was slightly lower than that in the wild-type-expressing cells. In contrast, the CL3B/SA- or the Δ2384-2433-mutated NS5A coimmunoprecipitated with the core protein only slightly or not at all.

We further examined the interaction of NS5A with core protein in cells expressing HCV genomes. At 72 h posttransfection with the wild type or CL3B/SA, cells were harvested and immunoprecipitated with an anti-NS5A antibody or an anti-C/EBPβ antibody as a negative control, followed by immunoblotting. Under these experimental conditions, the amount of extracellular core protein released from cells transfected with the CL3B/SA genome was about 10-fold lower than

that for the wild type, although comparable amounts of intracellular core protein were observed in both transfectants (Fig. 4B, left panels). As shown in the right panels of Fig. 4B, the core protein was specifically coimmunoprecipitated with NS5A in cells expressing the wild-type JFH-1 genome but not with the mutated NS5A in cells expressing the CL3B/SA genome. These results demonstrate that NS5A interacts with the core protein in cells producing infectious particles and that serine residues at aa 2428, 2430, and 2433 are important to the success of this interaction.

Two serine residues among aa 2428, 2430, and 2433 are responsible for regulating the interaction of NS5A with the core protein as well as HCV particle production. To further determine the critical residues in the C-terminal serine cluster of NS5A responsible for HCV particle production, we replaced one or two serine residues in the region with alanine (Fig. 1) and investigated which serine-to-alanine substitution influenced HCV particle production. Core protein levels in cells transfected with any construct were comparable over 4 days after transfection, indicating similar efficiencies of transfection and RNA replication from each construct (data not shown). As shown in Fig. 5A, we observed a slight delay in the kinetics of core protein release from cells transfected with the single-substitution genomes, S2428A, S2430A, and S2433A, up to 48 or 72 h posttransfection. However, core protein release from these cells reached comparable levels to that for the wild type at 96 h after transfection. In the cases of the double-substitution mutants (Fig. 5B), core protein release from cells transfected with the double-substitution genomes was markedly reduced, with 10- to 30-fold decreases compared to that for wild type observed. The kinetics of core protein release were similar to that for CL3B/SA.

Interaction of NS5A carrying single or double serine-to-alanine substitutions with the core protein was investigated by coimmunoprecipitation analysis using HA-tagged NS5A constructs. NS5A mutants carrying a single substitution were coimmunoprecipitated with the core protein (Fig. 5C), while none of the double-substitution NS5A mutants or the triple-substitution mutant, CL3B/SA, coimmunoprecipitated with the core protein (Fig. 5D). These results suggest that at least two serine residues in the C-terminal serine cluster of NS5A (aa 2428, 2430, and 2433) are necessary for the interaction between NS5A and the core protein as well as for regulation of HCV particle production and that there is positive correlation between their interaction and the amount of core protein released.

Glutamic acid partially substitutes for serine phosphorylation in the interaction of NS5A with the core protein and virus production. A consequence of phosphorylation is the addition of negative charge to a protein. In some cases, phosphoserine can be mimicked by glutamic or aspartic acid (14). To determine whether the introduction of negative charges into aa 2428, 2430, and 2433 instead of phosphoserines positively regulates the interaction of NS5A with the core protein and virus production, we replaced the serine residues with glutamic acid residues and constructed the CL3B/SE and S2428/2430E mutants (Fig. 6A). Cells transfected with the double-glutamic acid substitution, S2428/2430E, exhibited similar kinetics to the wild-type-transfected cells and released ~22-fold more core protein than S2428/2430A-transfected cells by 96 h posttransfection (Fig. 6B). In contrast,

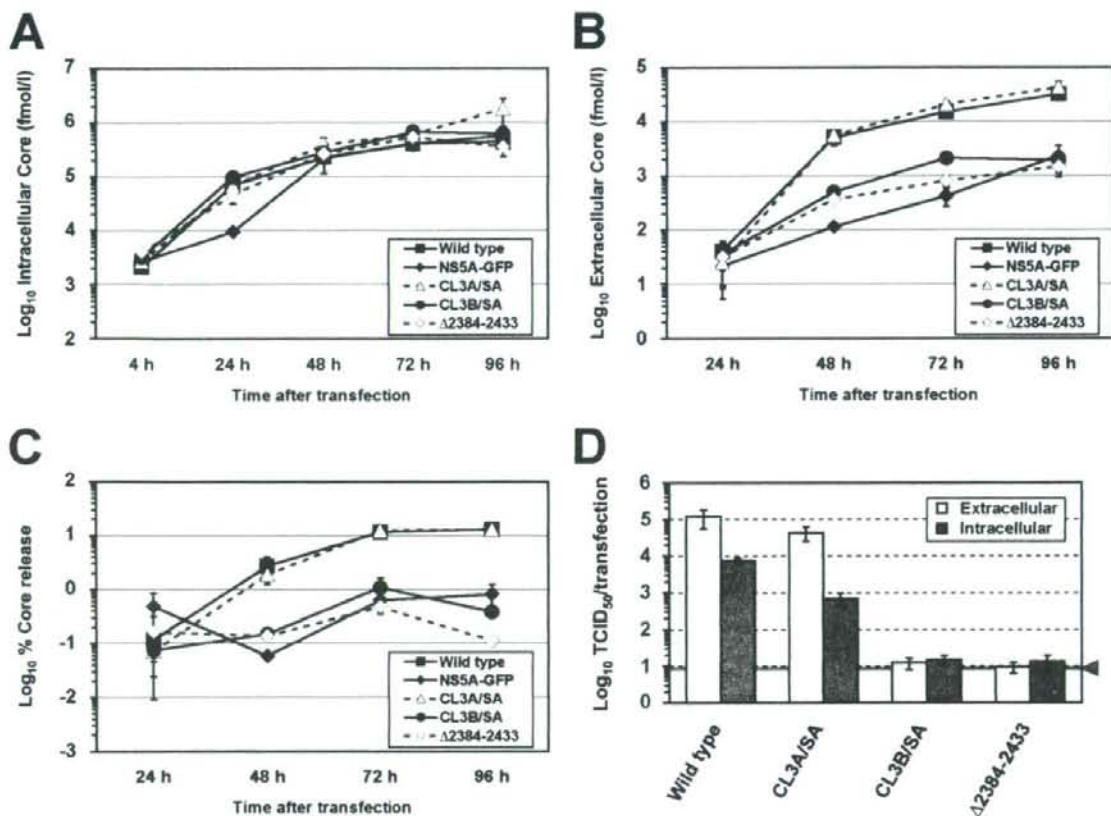


FIG. 3. Effect of mutations introduced into the NSSA C terminus on the production of infectious HCV particles. (A) Intracellular levels of core protein measured at various time points after transfection. A total of 3×10^6 Huh-7 cells were transfected with 10 μ g of in vitro-transcribed HCV RNAs specified in the inset and resuspended in 10 ml of culture medium, after which 2-ml aliquots were seeded into each well of a six-well culture plate. The cells were harvested at different time points between 4 h and 96 h posttransfection, and then 500 μ l of cell lysate per well was prepared. After centrifugation, supernatants were processed for a core protein-specific ELISA. (B) Release of core protein from cells transfected with the HCV genomes specified in the inset. Cell culture supernatants harvested from cells given in panel A were analyzed by a core protein ELISA. (C) Efficiency of core protein release from cells transfected with the HCV genomes specified in the inset. The percent core protein release (vertical axis) indicates the percentage of released core protein in relation to total core protein (the sum of intra- and extracellular core protein) calculated for each time point. (D) Infectivity of virus particles contained in supernatants and cells after transfection with mutants specified below the graph. Culture supernatants and cells were harvested 72 h posttransfection, and extracellular (white bars) and intracellular infectivity (gray bars) levels were determined by TCID₅₀ assay. The gray line and arrowhead represent the detection limit of the limiting dilution assay. Mean values and standard deviations for at least triplicates are shown in all panels.

the transfectant with the triple glutamic acid substitution, CL3B/SE, showed similar trends to that of CL3B/SA. In the coimmunoprecipitation experiments with FLAG-tagged core protein and HA-tagged NSSA constructs (Fig. 6C), S2428/2430E, but not S2428/2430A, restored the ability of NSSA to interact with the core protein up to a similar level to that of wild type. As expected, neither CL3B/SE nor CL3B/SA coimmunoprecipitated with the core protein. Taken together, these results indicate that negative charges at aa 2428 and 2430 preserve the ability of NSSA to interact with the core protein and positively regulate virus production. However, the data of the CL3B/SE mutant indicate that it is likely that negative charges alone are not sufficient to enhance either the interaction of NSSA with the core protein or virus production.

Subcellular localization of NSSA and core protein in Huh-7 cells expressing HCV genomes. The coimmunoprecipitation experiments described above indicate that the wild-type NSSA but not the CL3B/SA mutant interacts with the core protein. To evaluate the NSSA-core protein interaction in intact cells, we examined the subcellular localization of NSSA with the core protein by immunofluorescence analysis. NSSA colocalized with the core protein in cells transfected with the JFH-1 wild type (Fig. 7A), whereas their colocalization was rarely observed in cells transfected with the CL3B/SA RNA (Fig. 7B).

To further analyze the subcellular compartments for the localization of NSSA and core protein in cytoplasmic membrane structures, including the endoplasmic reticulum (ER) and LDs, we performed subcellular fractionation studies as

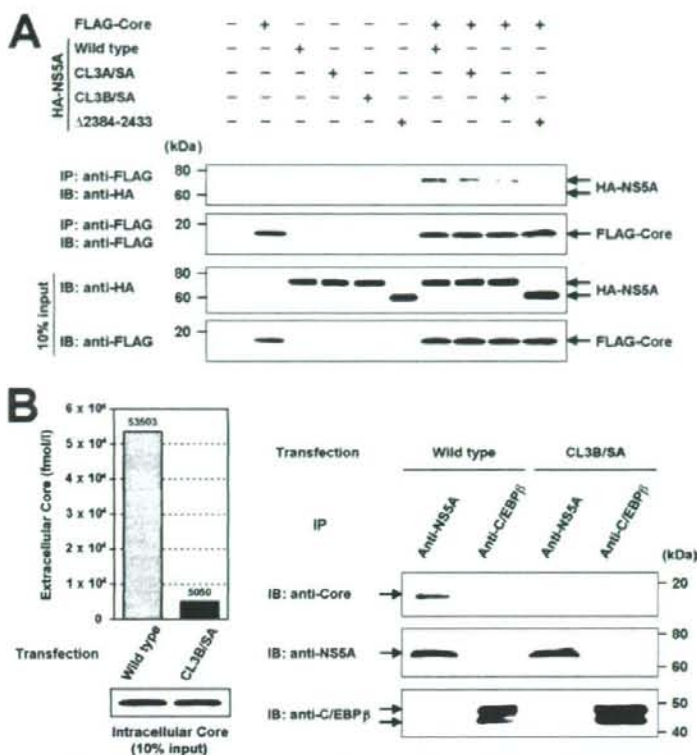


FIG. 4. aa 2428, 2430, and 2433 are essential for the interaction between NS5A and the core protein. (A) Effect of mutations at the NS5A C terminus on the interaction of NS5A with the core protein. N-terminally FLAG-tagged core protein and N-terminally HA-tagged NS5A carrying defined mutations were coexpressed in Huh-7 cells and immunoprecipitated with anti-FLAG antibody. The resulting precipitates were examined by immunoblotting using anti-HA or FLAG antibody. One-tenth of the cell lysates used in IP is shown as the 10% input. (B) Interaction between NS5A and the core protein in HCV-replicating cells. Huh-7 cells were lysed 72 h after transfection of the in vitro transcript of the HCV genome (wild type or CL3B/SA) and were immunoprecipitated with anti-NS5A antibody or anti-C/EBPβ antibody as a negative control. The resulting precipitates were examined by immunoblotting using anti-core protein, NS5A, or C/EBPβ antibody. One-tenth of cell lysates used in IP was immunoblotted with anti-core protein antibody (10% input). Cell culture supernatants harvested from transfected cells were analyzed by a core protein ELISA in parallel. IB, immunoblotting.

described in Materials and Methods. The iodixanol gradient was collected from the top to the bottom into 12 fractions (fractions 1 to 12). As shown in Fig. 7C, an ER marker, calnexin, was found in fractions 7 to 12 and was localized primarily in fractions 11 and 12. In contrast, ADRP, a cellular marker for LDs, was mainly observed in fractions 4 to 7. These two markers were equally distributed among cells analyzed (data not shown). The distribution of the wild-type NS5A was found in fractions 4 to 7, which was parallel to the fractionation profile of ADRP. The CL3B/SA-mutated NS5A was more broadly distributed and was also observed in heavier fractions than the wild-type NS5A, which was analogous to distribution of NS5A expressed in JFH1/4-1 cells bearing subgenomic replicons. The core protein in cells expressing the JFH-1 wild type, the CL3B/SA mutant, and in Huh/c-p7 cells that express JFH-1 structural proteins was distributed in a similar fashion, indicating that the distribution of core protein is not affected by NS5A mutation. The fractionation profile of the core protein, with a peak in fraction 4 or 5, was similar to that of the wild-type

NS5A or ADRP but not to that of the CL3B/SA-mutated NS5A or calnexin, suggesting that core protein interacts with the wild-type NS5A in LD fractions, which is consistent with previous reports (33, 44, 45).

NS5A-core protein interaction is important for association of the core protein with the viral genomic RNA. To further address our hypothesis regarding involvement of NS5A in recruiting viral RNA to nucleocapsid formation, we analyzed the association of the core protein with HCV RNA in wild-type- or CL3B/SA-expressing cells by IP-RT-PCR (Fig. 8). Both cell lysates were immunoprecipitated with an anti-core protein antibody or a negative control, mouse IgG. Total RNA prepared from each immunoprecipitate was subjected to RT-PCR in order to detect HCV RNA. The amounts of immunoprecipitated core protein (Fig. 8, lower panel) as well as the expression of HCV RNA (Fig. 8, upper panels, Input) were comparable in both cells. In cells expressing the wild-type JFH-1 genome, the viral RNAs covering the 5' terminal 2.2-kb as well as the 3' terminal 2.2-kb regions were detected in immunopre-

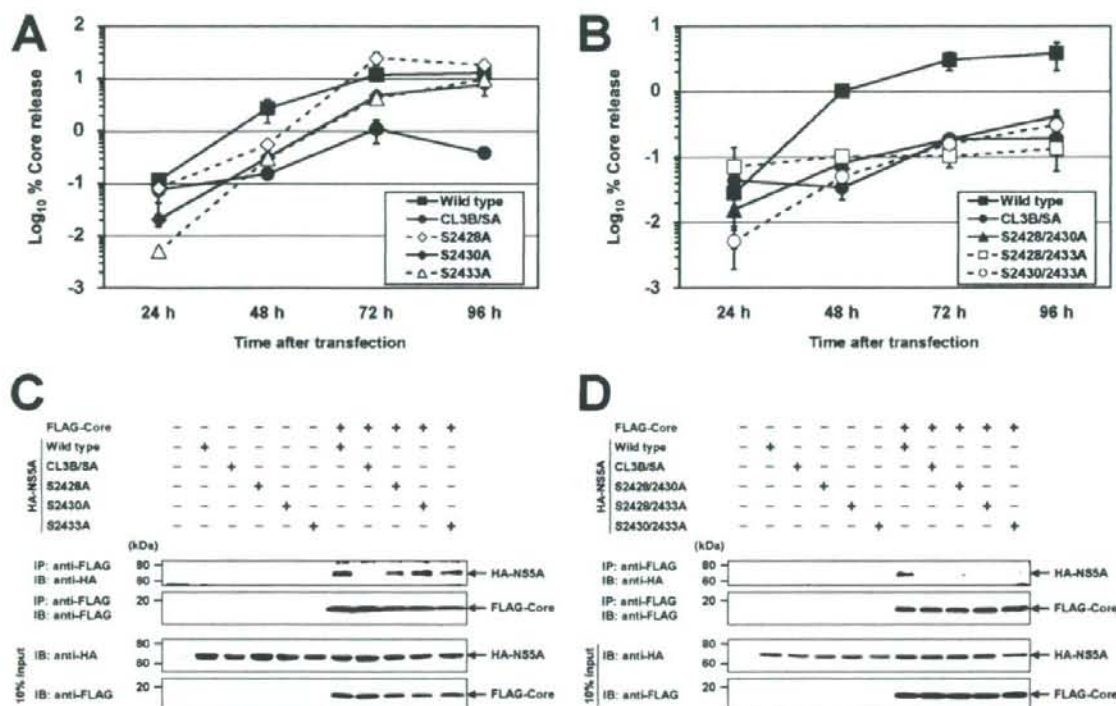


FIG. 5. Determination of critical amino acids responsible for virus production and the interaction of NS5A with the core protein. (A and B) Effect of single or double serine-to-alanine substitutions on virus production. After transfection of *in vitro* transcripts of the HCV genomes specified in the inset into Huh-7 cells, the cells and culture supernatants were harvested at the time points given, and the amounts of the core protein were determined by core protein-specific ELISA. Percent core protein release (vertical axis) indicates the percentage of released core protein in relation to total core protein (the sum of intra- and extracellular core protein) calculated for each time point. Mean values and standard deviations for at least triplicate experiments are shown. (C and D) Effect of single or double serine-to-alanine substitutions on the interaction between NS5A and the core protein. N-terminally FLAG-tagged core protein and N-terminally HA-tagged NS5A carrying defined mutations were coexpressed in Huh-7 cells and immunoprecipitated with anti-FLAG antibody. The resulting precipitates were examined by immunoblotting using anti-HA or FLAG antibody. One-tenth of the cell lysates used in IP is shown as the 10% input. IB, immunoblotting.

precipitates obtained with the anti-core protein antibody but not with the mouse IgG. In contrast, in cells expressing the CL3B/SA genome, HCV RNA was not detected in the immunoprecipitates with either antibody. These results demonstrate that HCV RNA associates with the core protein in cells where NS5A interacts with core protein (JFH-1 wild type) but not in cells where their interaction is impaired (CL3B/SA).

DISCUSSION

In the present study, we demonstrated the involvement of NS5A in the production of HCV particles via the interaction of NS5A with the core protein and identified its C-terminal serine cluster 3-B (aa 2428, 2430, and 2433), which is implicated in basal phosphorylation, as a key element for the interaction of NS5A with the core protein and for infectious virus production. Serine-to-alanine substitutions at the cluster, which have no impact on viral RNA replication, inhibit the interaction between NS5A and the core protein, thereby indicating that there is a connection between NS5A-core protein association and virus production. Finally, CL3B mutation leads to impair-

ment of the association of the core protein with HCV RNA and, therefore, possibly RNA encapsidation.

Several reports have indicated that viral NS proteins are involved in the virion assembly of *Flaviviridae* viruses (25, 29, 30, 33). For instance, mutations in yellow fever virus NS2A block production of infectious virus, and this perturbation can be released by a suppressor mutation in NS3 (25), while the hydrophobic residues of Kunjin virus NS2A required for virus assembly have been mapped (26). Miyanari et al. have shown that HCV core protein recruits NS proteins to the LD-associated membranes and that the NS proteins around the LDs participate in the assembly of infectious viral particles (33). Furthermore, during preparation of the current article, two studies regarding participation of NS5A in the assembly of HCV particles were published. Appel et al. have demonstrated the essential role of domain III of NS5A in the formation of infectious particles, and deletions in this domain that disrupt colocalization of NS5A and the core protein abrogate virion production (2). Tellinghuisen et al. identified a serine residue in domain III as a key determinant for viral particle production